$^{87}Sr/^{86}Sr$ AS A POTENTIAL FINGERPRINT FOR DETERMINING THE PROVENANCE OF TOTAL DISSOLVED SOLIDS ASSOCIATED WITH HYDRAULIC FRACTURING ACTIVITIES IN THE BARNETT SHALE, TEXAS

by

RICHARD BRIAN GOLDBERG

Presented to the Faculty of the Graduate School of

The University of Texas at Arlington in Partial Fulfillment

of the Requirements

for the Degree of

MASTER OF SCIENCE IN ENVIRONMENTAL AND EARTH SCIENCES

THE UNIVERSITY OF TEXAS AT ARLINGTON

May 2016

Acknowledgements

I would like to thank my thesis advisor, Dr. Elizabeth Griffith for all of her support and mentorship. This thesis would never have happened without her guidance and desire to push me to achieve. I would also like to thank my thesis committee for their knowledge and assistance during this process.

I would like to thank the faculty at The University of Texas at Arlington from whom I studied and grew as a geoscientist. It is with their superb instruction that I was enabled to successfully complete my coursework.

I would like to thank my family and my girlfriend, Stephanie for their support while allowing me to go back to school to follow a dream studying a subject I find fascinating. I would never have been able to do it without all of them. They allowed me the time to do this giving their patience and understanding, as I often had to prioritize my studies over spending quality time with them.

I would like to thank peers from my coursework and Dr. Griffith's lab group who took time out of their day to listen to multiple presentations and provide quality feedback.

April 22, 2016

Abstract

$^{87}Sr/^{86}Sr$ AS A POTENTIAL FINGERPRINT FOR DETERMINING THE PROVENANCE OF TOTAL DISSOLVED SOLIDS ASSOCIATED WITH HYDRAULIC FRACTURING ACTIVITIES IN THE BARNETT SHALE, TEXAS

Richard Goldberg, M.S.

The University of Texas at Arlington, 2016

Supervising Professor: Elizabeth M. Griffith

Over the last decade there has been a dramatic increase in unconventional drilling that utilizes hydraulic fracturing to extract oil and gas. The Barnett Shale in north central Texas has been a significant contributor to this increase in unconventional production. Potential environmental contamination from hydraulic fracturing and associated activities is a topic of current debate. One concern is the management of produced/flowback water (PFW), which contains high amounts of total dissolved solids (TDS) acquired from interaction with the reservoir formation and its constituents. Development and testing of geochemical methods to determine if a particular contaminant is the result of PFW or natural sources would be valuable to industry. $^{87}Sr/^{86}Sr$ analysis has been shown to be a promising method for determining the provenance of TDS due to the wide variation seen naturally in $^{87}Sr/^{86}Sr$ on both large and small spatial scales, low temporal variability over the life of a well, and the lack of changes in $^{87}Sr/^{86}Sr$ during evaporation. Samples acquired from different sources, such as groundwater and PFW can contain unique $^{87}Sr/^{86}Sr$ values. The mixing of these two end-members will produce a curve that can verify the amount and source of a

contaminant. The results of the study produced a mixing curve with end members composed of a contaminant (PFW), containing relatively high Sr concentrations and $^{87}Sr/^{86}Sr$, and an "uncontaminated" sample (aquifer), containing relatively low concentrations of Sr and $^{87}Sr/^{86}Sr$. The curve shows that when as little as 1% of this mixture is flowback, the "uncontaminated" sample experiences a measureable change in $^{87}Sr/^{86}Sr$. To determine which phase within the reservoir rock imparts its $^{87}Sr/^{86}Sr$ to the PFW, sequential extractions using water, ammonium acetate, acetic acid, and hydrochloric acid (HCl) were performed on powdered core samples sourced from the Barnett Shale. Sodium was preferentially extracted with water, representing soluble salts. Barium and potassium were found primarily in exchangeable sites (ammonium acetate). Calcium and strontium were found primarily in both exchangeable sites and carbonate, and magnesium was primarily in the carbonate and HCl soluble leaches. Measurements of $^{87}Sr/^{86}Sr$ performed on these leachates indicate that the different phases within the shale contain distinct $^{87}Sr/^{86}Sr$ values. It was expected that the water leachate would provide a similar ratio of $^{87}Sr/^{86}Sr$ to flowback based on the assumption that it is a reasonable approximation of hydraulic fracturing fluid interacting with shale or its formation fluids. Analysis of the results indicates this might not be the case. However, the study was hindered by a limited sample set with one critical variable being unknown: whether or not the core samples and flowback sample are sourced from the same location. This is imperative to fully compare and contrast the samples. For example, flowback samples sourced from hydraulic fracturing activities in the Marcellus Shale, Pennsylvania has been shown to vary widely by collection site (Chapman et al., 2012; Capo et al., 2013). Therefore, further work should be done using this sequential extraction technique with samples (shale cuttings and flowback) sourced from the same well location.

Table of Contents

Acknowledgements.....iii

Abstract.....iv

List of Illustrations.....viii

List of Tables.....x

Chapter 1 Introduction.....1

1.1 Purpose of Research.....1

1.2 Hydraulic Fracturing.....1

1.3 Hydraulic Fracturing Within the Barnett Shale.....3

1.4 Environmental Concerns Regarding Hydraulic Fracturing.....8

1.5 Radiogenic Strontium.....12

1.6 Prior Research - $^{87}Sr/^{86}Sr$ as a Geochemical Tracer.....14

1.7 Mixing Curve.....16

1.8 Hypothesis.....18

Chapter 2 Study Site.....20

2.1 Stratigraphy.....20

2.2 Geochemical Background.....25

Chapter 3 Methods.....28

3.1 Sample Collection.....28

3.2 Procedures.....30

Chapter 4 Results.....39

4.1 Sequential Extractions.....39

4.2 Aquifer Samples.....45

4.3 Flowback Sample.....46

Chapter 5 Discussion.....48
5.1 Carbonate Mineralogy in the Barnett Shale.....48
5.2 Comparison of Barnett Shale Leachates to Flowback.....52
5.3 Comparison of Aquifer Samples to Flowback.....56
Chapter 6 Conclusions.....60
Appendix A Extraction Chromatography Procedure.....63
Appendix B Sequential Extraction Procedure.....64
References.....65
Biographical Information.....73

List of Illustrations

Figure 1-1 Map of hydrocarbon wells in the Barnett Shale as of 2011.....4

Figure 1-2 Decline in price of WTI from 2006-2016.....5

Figure 1-3 Oil and gas production in the Barnett Shale between 2006-2015.....6

Figure 1-4 Rig counts in the Barnett Shale from 2011-2015.....7

Figure 1-5 Drilling permits issued in the Barnett Shale from 2006-2015.....7

Figure 1-6 Cartoon of a typical well bore showing potential routes for a fluid leak.....9

Figure 1-7 Different types of casing/cement failure in a wellbore.....10

Figure 1-8 Breakdown of 1144 notices of violation issued by PDEP.....10

Figure 1-9 Cartoon of strontium cycle.....14

Figure 1-10 $^{87}Sr/^{86}Sr$ values of flowback samples within the Marcellus Shale.....15

Figure 1-11 $^{87}Sr/^{86}Sr$ values of Marcellus flowback samples by county.....16

Figure 1-12 Evaporation-mixing model between flowback and surface waters.....18

Figure 2-1 Generalized stratigraphic column of the study area.....21

.

Figure 2-2 Generalized change in stratigraphy within the DFW Metroplex.....22

Figure 2-3 Isopach maps of Barnett Shale and Forestburg Limestone.....22

Figure 2-4 Map of the study area showing Barnett Shale and local aquifers.....24

Figure 3-1 Powdered Barnett Shale core samples used in study.....30

Figure 3-2 Picture of 125 µL Teflon column used in study.....35

Figure 3-3 Results of extraction chromatography, 2/25/15.....36

Figure 4-1 Fractions of elements leached by each sequential extraction.....43

Figure 5-1 Comparison of molar (Fe+Mg)/(Fe+Mg+Ca) of leached samples.....49

Figure 5-2 Mineralogy of Forestburg Limestone and lower Barnett Shale.....51

Figure 5-3 Comparison of molar fractions by leachate for core samples.....54

Figure 5-4 $^{87}Sr/^{86}Sr$ of the Barnet Shale leachates compared to flowback sample…...56

Figure 5-5 Mixing line between the measured aquifer and flowback end members…..59

List of Tables

Table 1-1 Partial list of additives to proppants used in fracturing fluid.....2

Table 2-1 TDS and metal concentrations in wells surrounding the Barnett Shale.....27

Table 3-1 List of private well samples used in study.....29

Table 3-2 List of standards used for analysis on ICP-OES.....32

Table 3-3 Amount of elemental standards used to create high standard.....33

Table 3-4 Amount of elemental standards used to create medium standard.....33

Table 3-5 Amount of elemental standards used to create low standard.....33

Table 3-6 Wavelengths used for analysis on ICP-OES.....34

Table 3-7 Leachates analyzed and analysis of SRM 987 for run 1 on MC-ICPMS.....37

Table 3-8 Leachates analyzed and analysis of SRM 987 for run 2 on MC-ICPMS.....38

Table 4-1 Element concentrations in leachates of Barnett Shale core cuttings.....40

Table 4-2 Calculated total carbonate wt % from acetic acid leach by sample……..43

Table 4-3 $^{87}Sr/^{86}Sr$ of Barnett Shale core samples by sequential extraction…….44

Table 4-4 Elemental concentrations and $^{87}Sr/^{86}Sr$ of the aquifer (well) samples.....47

Table 4-5 Elemental concentrations and $^{87}Sr/^{86}Sr$ of the flowback sample.....47

Table 5-1 Molar (Mg+Fe)/(Mg+Fe+Ca) of Ac and HCl leach……..50

Chapter 1

Introduction

1.1 Purpose of Research

The purpose of this thesis project is to determine the viability of utilizing radiogenic strontium ($^{87}Sr/^{86}Sr$) to identify the provenance of total dissolved solids (TDS) associated with hydraulic fracturing activities, within the region overlying the Barnett Shale. Beginning in 2002, the Barnett Shale saw a dramatic increase in unconventional gas and oil production utilizing hydraulic fracturing. Many of these wells are in close proximity (<5 km) to private and agricultural sources of groundwater. Previous studies have suggested contamination of natural waters due to unconventional drilling operations (Osborn et al., 2011; Chapman et al., 2012; Fontenot et al., 2013; Vidic et al., 2013; Darrah et al., 2014; Rostron and Arkadakskiy, 2014; Vengosh et al., 2014; Warner et al., 2014; Brantley, 2015; Hildenbrand et al., 2015). In this study, $^{87}Sr/^{86}Sr$ will be measured from samples of groundwater (private wells), flowback water from hydraulic fracturing activities, and sequential extractions from Barnett Shale core samples to determine how $^{87}Sr/^{86}Sr$ varies among these different fluids. If they differ significantly, then it would be possible to constrain these values to their particular source like a fingerprint, giving the ability to identify a dissolved contaminant's origin. This method could then be utilized to potentially attribute or dismiss a claim that hydraulic fracturing activities were the cause of a contamination event.

1.2 Hydraulic Fracturing

Unconventional oil and gas is extracted from impermeable strata, which contain hydrocarbons trapped in their pore spaces. In order to free the hydrocarbons, hydraulic fracturing is utilized to break up the rock, increasing permeability. Hydraulic fracturing

includes the use of fracturing fluids composed of water and a proppant (typically sand) to invade the fractured cracks in order to maintain this newly created permeability. In addition, an assortment of chemicals is added to the fracturing fluid for a variety of purposes (Table 1-1).

Table 1-1. Partial list of additives to proppants used in hydraulic fracturing and their purpose

Additive type	Example compounds	Purpose
Acid	Hydrochloric acid	Clean out the wellbore, dissolve minerals, and initiate cracks in rock
Friction reducer	Polyacrylamide, petroleum distillate	Minimize friction between the fluid and the pipe
Corrosion inhibitor	Isopropanol, acetaldehyde	Prevent corrosion of pipe by diluted acid
Iron control	Citric acid, thioglycolic acid	Prevent precipitation of metal oxides
Biocide	Glutaraldehyde, 2,2-dibromo-3-nitrilopropionamide (DBNPA)	Bacterial control
Gelling agent	Guar/xantham gum or hydroxyethyl cellulose	Thicken water to suspend the sand
Crosslinker	Borate salts	Maximize fluid viscosity at high temperatures
Breaker	Ammonium persulfate, magnesium peroxide	Promote breakdown of gel polymers
Oxygen scavenger	Ammonium bisulfite	Remove oxygen from fluid to reduce pipe corrosion
pH adjustment	Potassium or sodium hydroxide or carbonate	Maintain effectiveness of other compounds (such as crosslinker)
Proppant	Silica quartz sand	Keep fractures open
Scale inhibitor	Ethylene glycol	Reduce deposition on pipes
Surfactant	Ethanol, isopropyl alcohol, 2-butoxyethanol	Decrease surface tension to allow water recovery

(From Vidic et al., 2013).

A large percentage of this fracturing fluid remains within the formation (typically 60%-80%), while a portion returns to the surface, called flowback ("Difference between flowback and produced water", 2011). This flowback water is a combination of the original fracking fluid and any TDS that it has acquired from its interaction with the formation directly or formation fluids. Flowback can last up to 3 to 4 weeks, with the majority returning in the first 7 to 10 days after injection of the fracking fluid. Any water that is

returned to the surface from the well after the flowback period is called produced water. Produced water is naturally occurring water found in situ within the formation, which contains high amounts of TDS and will continue to return to the surface over the life of the well ("Difference between flowback and produced water", 2011).

1.3 Hydraulic Fracturing Within the Barnett Shale

Advances in technology, with an accompanying increase in the price of oil, led to a boom in the exploration and drilling of unconventional reservoirs. In the United States between 1990 and 2011 the contribution of unconventional gas to total gas production went from negligible levels to 30% (Vidic et al., 2013). The U.S. Dept. of Agriculture has projected that by 2035 approximately 50% of total gas production in the U.S. will come from unconventional reservoirs (Vengosh et al., 2013). The Barnett Shale located around Ft. Worth, Texas is drilled extensively for natural gas with far more unconventional wells then conventional (Fig. 1-1).

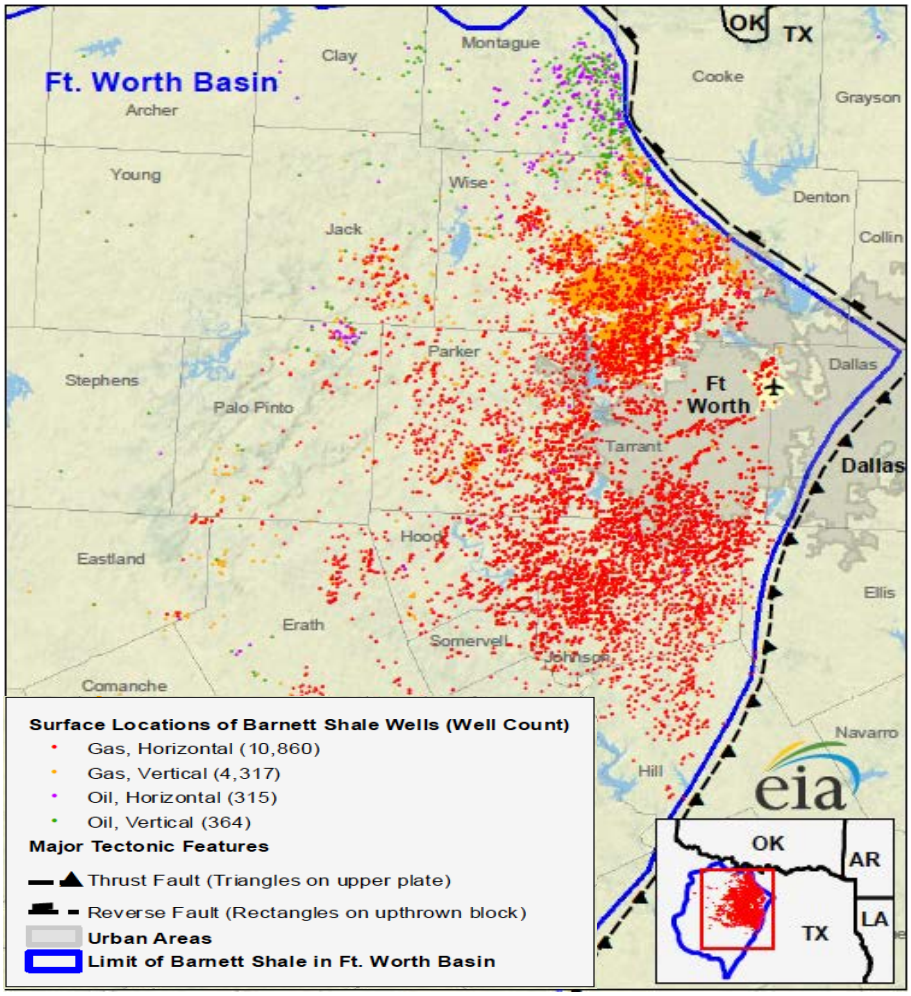

Figure 1-1. Map of hydrocarbon wells in the Barnett Shale as of 2011 showing red/purple sites (unconventional wells) far exceeding orange/green sites (conventional gas wells) ("Unconventional/conventional wells," 2011).

Beginning in 2014, the global price of oil began to decline and is currently lower than it has been in over a decade (Fig. 1-2). As a result, BBL (barrels of oil) and MCF (1000 cubic feet of gas) (Fig. 1-3), rig counts (Fig. 1-4), and applications for new drilling permits (Fig. 1-5) within the Barnett Shale declined concurrently with this drop in the price of hydrocarbons.

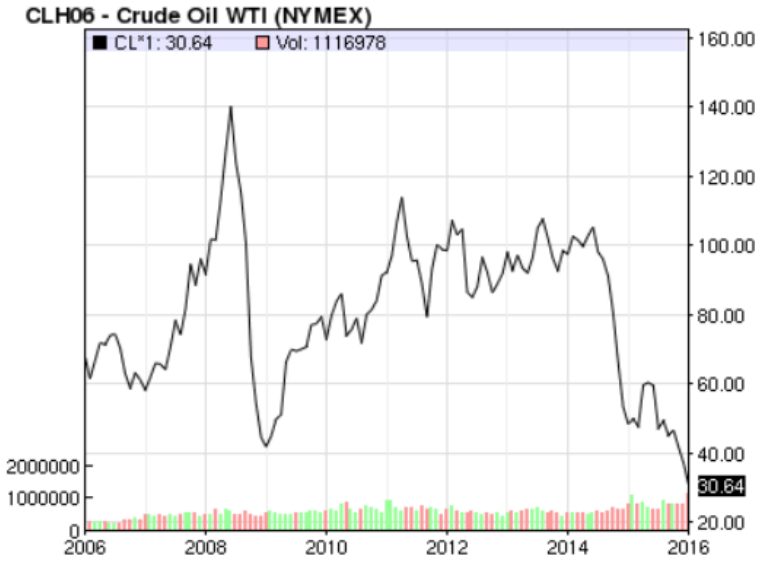

Figure 1-2. Decline in price of West Texas Intermediate (WTI) crude from 2006-2016. (“Price of oil,” 2016).

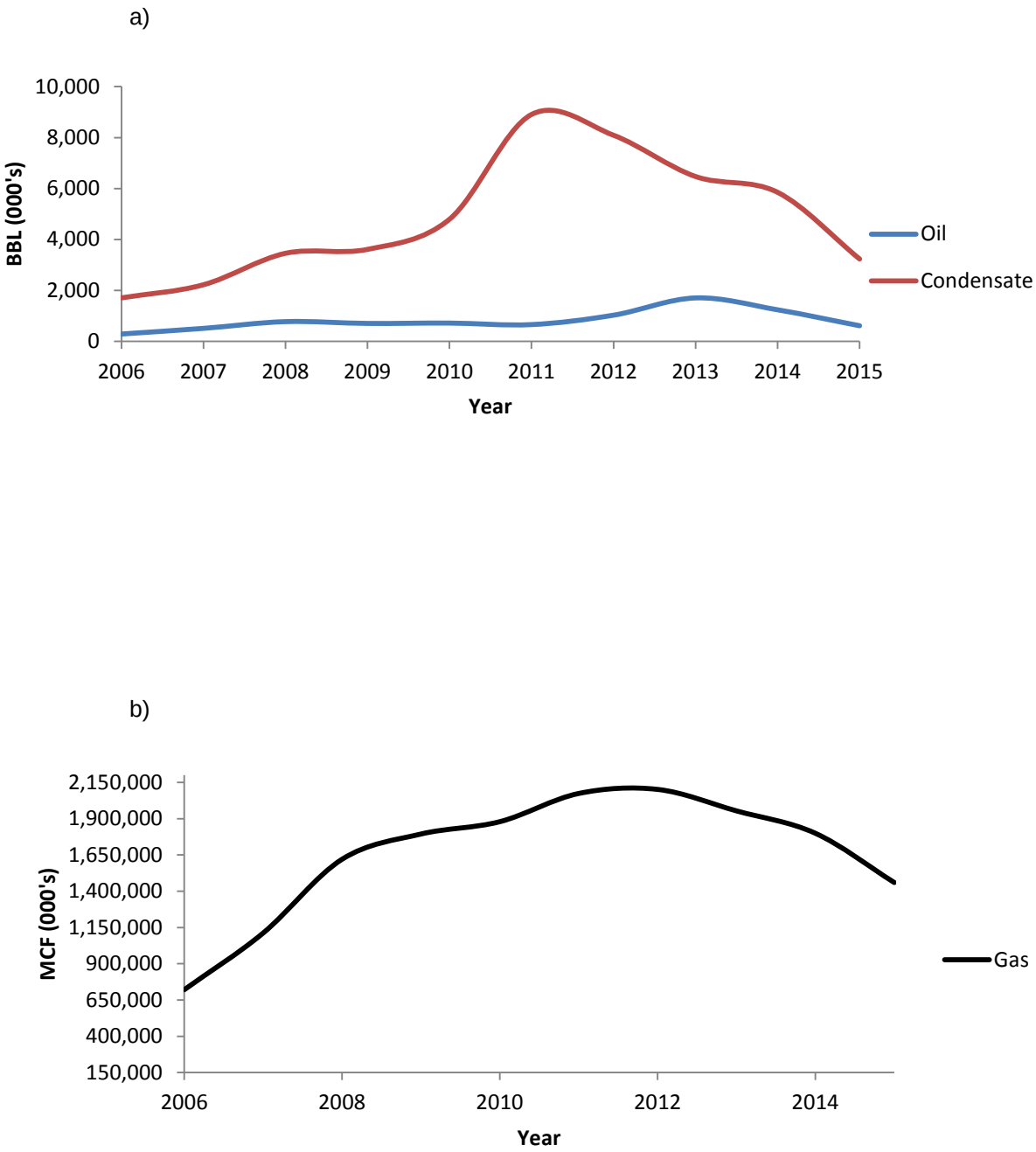

Fig. 1-3 a) Oil/Condensate (in thousands of BBL) and b) Gas Production (in thousands of MCF) between 2006-2015 from the Barnett Shale. Hydrocarbon production hit a peak in 2011 and has declined since. Data from TXRRC (2016).

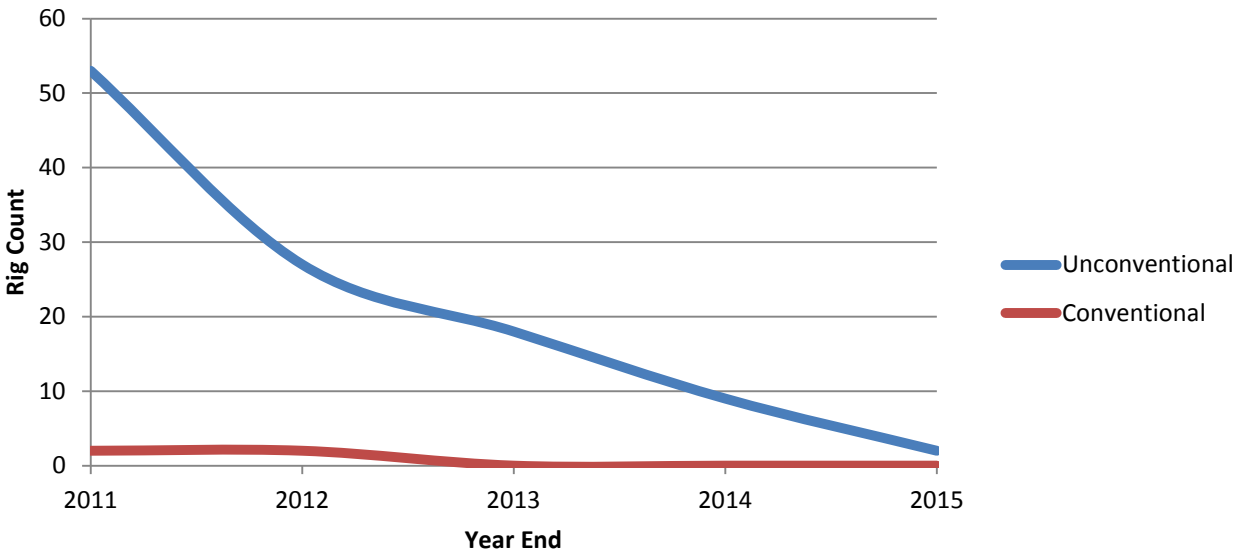

Figure 1-4. Rig counts within the Barnett Shale from 2011-2015 ("Barnett Shale rig counts," 2015).

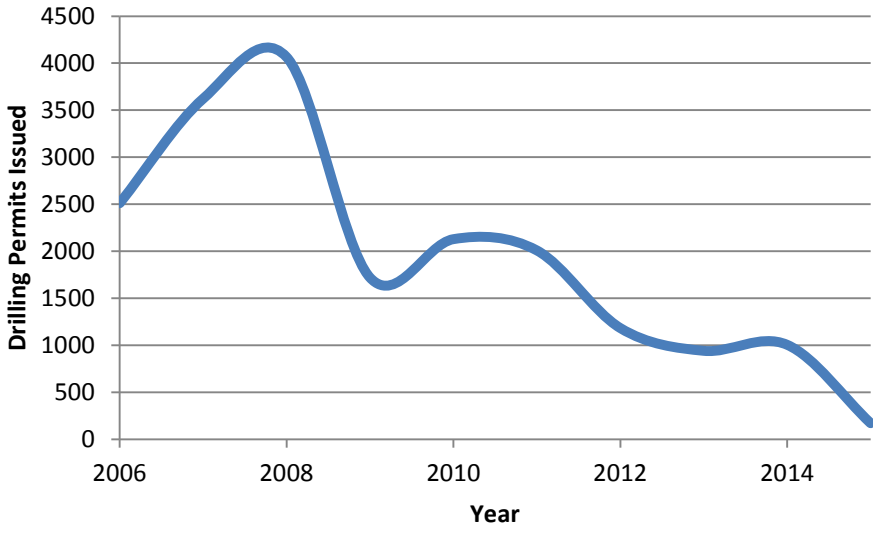

Figure 1-5. Drilling Permits issued within the Barnett Shale from 2006-2015. New permit requests peaked in 2007 and have dropped approximately 95% since 2007. Data from TXRRC (2016).

1.4 Environmental Concerns Regarding Hydraulic Fracturing

As with any resource extraction activity it is important to understand potential impacts to the surrounding environment. Previous studies have suggested contamination of natural waters due to unconventional drilling operations (Osborn et al., 2011; Chapman et al., 2012; Fontenot et al., 2013; Vidic et al., 2013; Darrah et al., 2014; Rostron and Arkadakskiy, 2014; Vengosh et al., 2014; Warner et al., 2014; Brantley, 2015; Hildenbrand et al., 2015). The greatest concerns regarding potential contamination from fracking activities are a result of casing leakage, well blowouts, and spills (Vidic et al., 2013). Casing failures occur as a result of the deterioration of the cement or steel casing surrounding the wellbore (Figs. 1-6 and 1-7) and other poor well completion practices (Davies et al., 2014). The Pennsylvania Department of Environmental Protection found construction violations in 219 out of 6466 hydrocarbon wells between 2008-2013, and discovered the casings are the primary culprits of wellbore failure when contamination from drilling activities has been confirmed (Vidic et al., 2013). Between 2011-2012, 2.58% of 3533 wells (1144 notices of violation) (Fig. 1-8) in Pennsylvania were identified as having some sort of casing or cement failure (Davies et al., 2014).

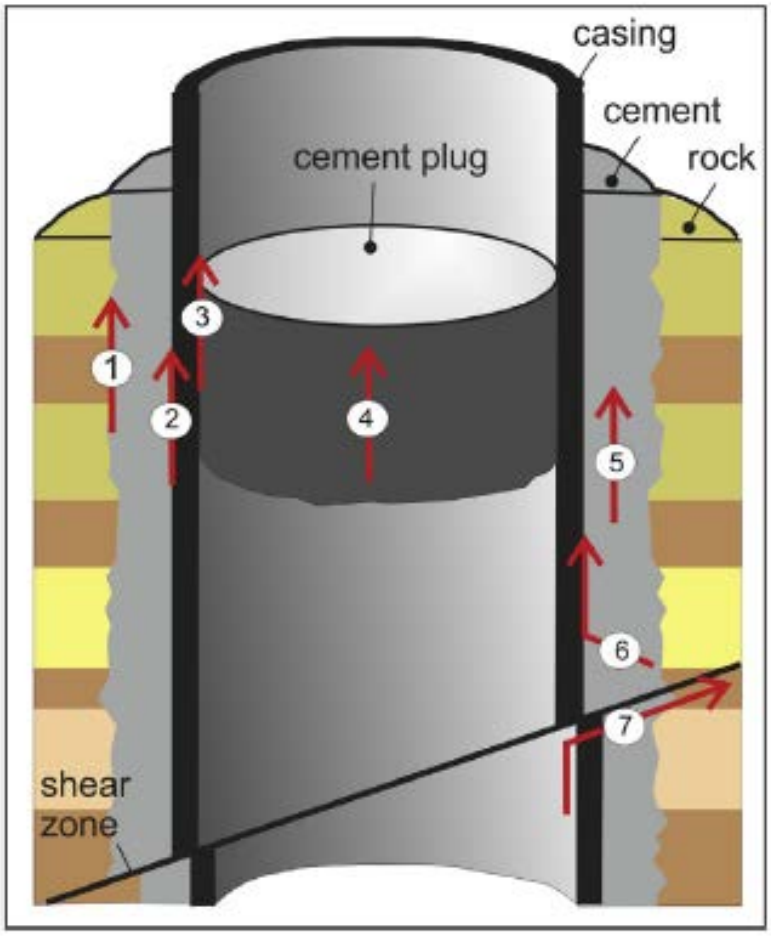

Figure 1-6. Cartoon of a typical well bore showing potential routes for a fluid leak. 1 - between cement and surrounding rock formation, 2 - between casing and surrounding cement, 3 - between cement plug and casing (if plugged), 4 - through cement plug (if plugged), 5 - through the cement between casing and rock formation, 6 - across the cement outside the casing and then between the cement and casing, 7 - along a sheared wellbore ([After Celia et al., 2015]; Davies et al., 2014).

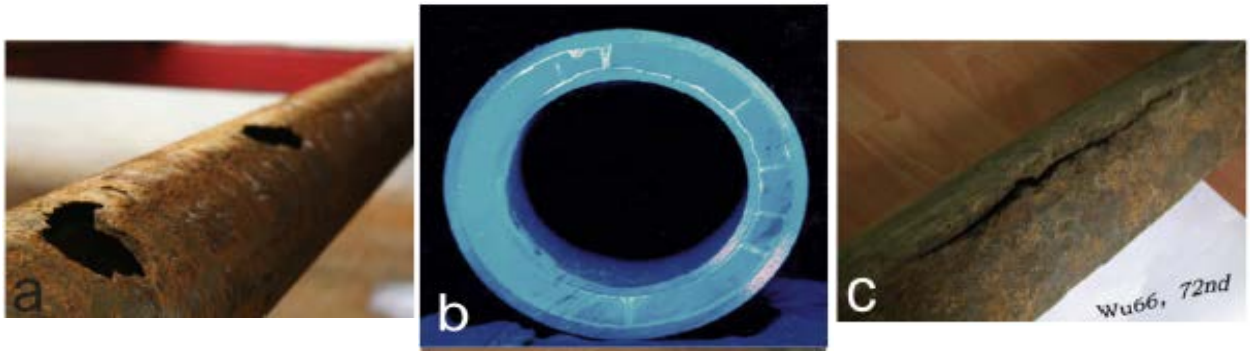

Figure 1-7. Different types of casing/cement failure in a wellbore. a) corrosion of tubing ([After Torbergsen et al., 2012]; Davies et al., 2014).), b) cracks in cement ([After Crook et al., 2003]; Davies et al., 2014). , c) corrosion of casing ([After Xu et al., 2006]; Davies et al., 2014).

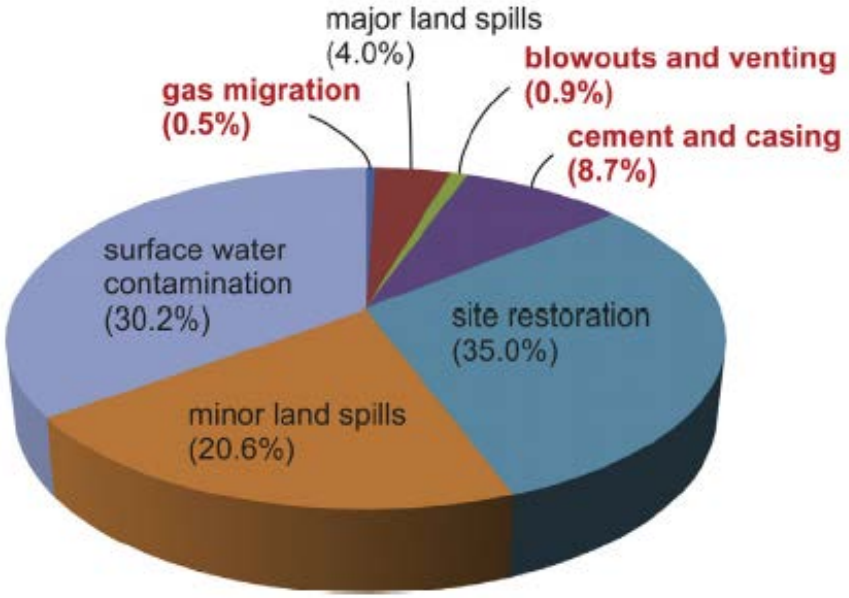

Figure 1-8. Breakdown of 1144 notices of violation issued by the Pennsylvania Department of Environmental Protection Text in red indicates instances of well barrier or integrity failure ([After Considine et al., 2013]; Davies et al., 2014).

Between 2005-2013 there were 24 incidents of influent/returned water spills or leaks with the largest of these incidents taking place in 2013, which involved the spillage of 200,000 gallons of fracking fluid within Washington township, Pennsylvania (Brantley et al., 2014; Brantley, 2015). Forty million people nationwide receive their drinking water from private wells (Vidic et al., 2013), some of which are in close proximity to hydraulic fracturing operations (Fontenot et al., 2013) making spills or leaks particularly concerning for ground and surface water quality. An examination of 60 private drinking wells across Pennsylvania and New York determined that average methane levels within 1 km of active gas extraction sites were elevated (17 times higher on average) as compared to wells in non-active areas, raising the question of whether these elevated levels are connected directly to drilling activities or are naturally occurring (Osborn et al., 2011). Drinking water from private wells located within 5 km of active drilling operations in the Barnett Shale revealed elevated mean levels of As (0.0126 µg/L) and TDS (585 mg/L) exceeding the EPA's Drinking Water Maximum Contaminant Levels of As (0.0100 mg/L) and TDS (500 mg/L) compared with lowered levels further away from drilling operations (Fontenot et al., 2013). Mean dissolved strontium concentration of these wells within 5 km of active drilling was 2.32 mg/L with a maximum value of 18.20 mg/L (Fontenot et al., 2013). The elevated levels were postulated to be a result of ground perturbations caused by drilling activities, which liberated scaling into the groundwater that had built up within the wells ([After Groat and Grimshaw, 2012]; Fontenot et al., 2013). The EPA does not currently have a limit for Sr concentrations in drinking water, though they have a health reference limit listed as 4.20 mg/L (Alfredo et al., 2014).

The combination of chemical changes to drinking wells found in proximity to hydraulic fracturing sites, cases of spills or leaks of contaminated fluids into surface water and instances of casing failure at well sites confirm that drilling activities do have the

potential to influence the local environment. Tools and techniques need to be available to determine the source of a potential contamination event. Elevated concentrations of a particular element in a private well do not provide a unique fingerprint for provenance identification of a contaminant. Analyzing radiogenic Sr isotope ratios as a fingerprint to determine the provenance of dissolved solids is a very promising method that is targeted in this research (e.g., Chapman et al., 2012; Peterman et al., 2012; Capo et al., 2013).

1.5 Radiogenic Strontium

The element strontium (Sr) is atomic number 38 on the periodic table and has four naturally occurring stable isotopes: ^{84}Sr, ^{86}Sr, ^{87}Sr, and ^{88}Sr. ^{87}Sr is radiogenic and is created through the emission of a negative beta (β) particle during radioactive decay of ^{87}Rb which has a half life of 48.8 billion years (Faure and Mensing, 2005). As a result, the ratio of radiogenic ^{87}Sr to stable ^{86}Sr increases very slowly over time.

"Fingerprinting" fluids refers to the complementary geochemical techniques used to differentiate ambient water (or gas) from a contaminated or migrated formation water or gas (Rostron and Arkadakskiy, 2014). Radiogenic strontium is a strong candidate for "fingerprinting" or determining provenance of a contaminant due to a variety of factors including: a wide range of variation on both large and small scales, low temporal variability, and high abundance (Bataille et al., 2012). Additionally, unlike oxygen and hydrogen stable isotopic compositions, $^{87}Sr/^{86}Sr$ will not change due to evaporation as Sr concentrations increase (Peterman et al., 2012).

The $^{87}Sr/^{86}Sr$ of marine deposits (such as the Barnett Shale) are influenced by a variety of factors including the $^{87}Sr/^{86}Sr$ of any parent rock deposited as sediments into the marine environment and the influence of the strontium cycle on the $^{87}Sr/^{86}Sr$ of seawater at the time of deposition (Fig. 1-9). $^{87}Rb/^{87}Sr$ will vary between parent rock

inputs due to geochemical processes that fractionate $^{87}Rb/^{87}Sr$ and ages of the strata. The fractionation occurs due to the two elements having an affinity for different minerals (Bataille et al., 2012). Sr will substitute readily for calcium (Ca) and rubidium (Rb) will substitute for potassium (K). These dissimilar affinities cause Sr and Rb to vary widely at both large scales (i.e., between the crust and mantle) and small scales (i.e., between rocks and minerals). As ^{87}Rb decays to ^{87}Sr within the strata, the varying abundances of ^{87}Rb and age of deposition cause formations to acquire a unique $^{87}Sr/^{86}Sr$ signature.

The strontium cycle (Fig 1-9) describes fluxes into the ocean from primary processes such as chemical weathering of continental rock (~0.712) and the addition of new oceanic crust at mid ocean ridges (~0.703). Secondary processes include carbonate flux between seawater/sediments, sea floor weathering, and diagenesis (Godderis and Francois, 1995). The present day $^{87}Sr/^{86}Sr$ of seawater is ~0.709, thus during times of heavy continental erosion the ratio of $^{87}Sr/^{86}Sr$ of seawater will increase, whereas during times of increased seawater spreading where production of new oceanic crust is being produced the $^{87}Sr/^{86}Sr$ of seawater will decrease. The Barnett Shale was deposited during Mississippian time and thus should reflect the $^{87}Sr/^{86}Sr$ of Mississippian seawater (~0.7078-0.7081) (Denison et al., 1998). Over time, secondary processes such as diagenesis caused by the introduction of externally derived fluids into the Barnett have played a role in altering its $^{87}Sr/^{86}Sr$ (Pollastro et al., 2007).

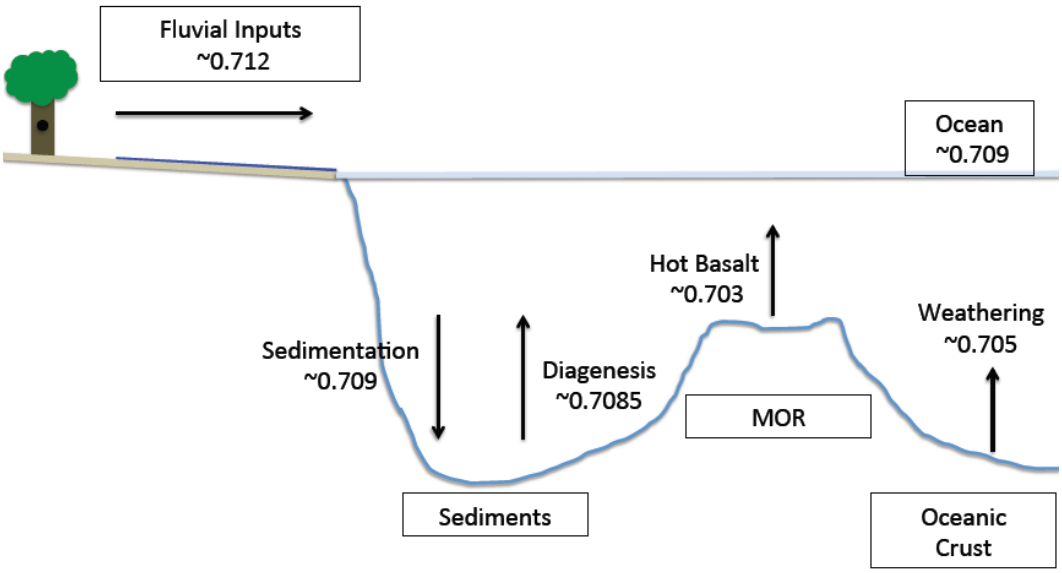

Figure 1-9. Cartoon of present day strontium cycle showing flux of $^{87}Sr/^{86}Sr$ into ocean from various inputs today. MOR= mid ocean ridge. (Modified from Godderis and Francois, 1995).

1.6 Prior Research - $^{87}Sr/^{86}Sr$ as a Geochemical Tracer

The Marcellus Formation in Pennsylvania has been drilled extensively for unconventional hydrocarbons. Capo et al. (2013) and Chapman et al. (2012) studied flowback and produced waters from drill sites within the Marcellus Shale gas play across multiple counties in Pennsylvania. Their combined analyses included flowback and produced waters from the commencement of drilling and up to two years after commencement. The results (Fig. 1-10) showed that the samples contained unique ranges of $^{87}Sr/^{86}Sr$ values particular to their source. This regional variance creates a constraint from which the original source of potential contaminants in a sample can be determined. Another result of the studies showed that the flowback and produced samples from the various well sites display the same overall trend (curvature) over time of both Sr concentration (mg/L) and the ratio of $^{87}Sr/^{86}Sr$ (Fig. 1-11). The total Sr

concentration in the samples increased over the entire first year of the study indicating a progressive incorporation of formation salts into the fracturing fluid and the resultant PFW. The ratio of $^{87}Sr/^{86}Sr$ increased over the first few days of drilling, quickly reaching a steady state value (Capo et al., 2013). The results of the studies validated the use of radiogenic Sr to constrain the source of constituents in a fluid. More research needs to be done to see if the same approach in the Marcellus Shale gas play can be applied to other regions of the globe.

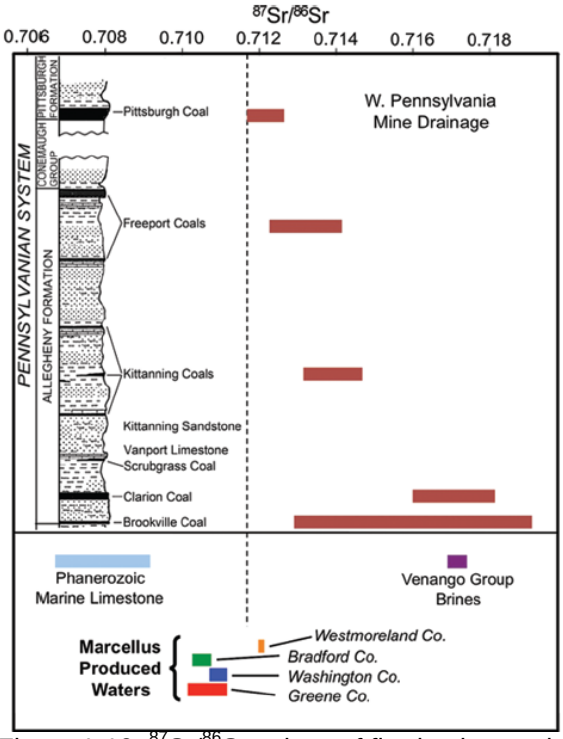

Figure 1-10. $^{87}Sr/^{86}Sr$ values of flowback samples within the Marcellus Shale gas play by county and formation (from Chapman et al., 2012).

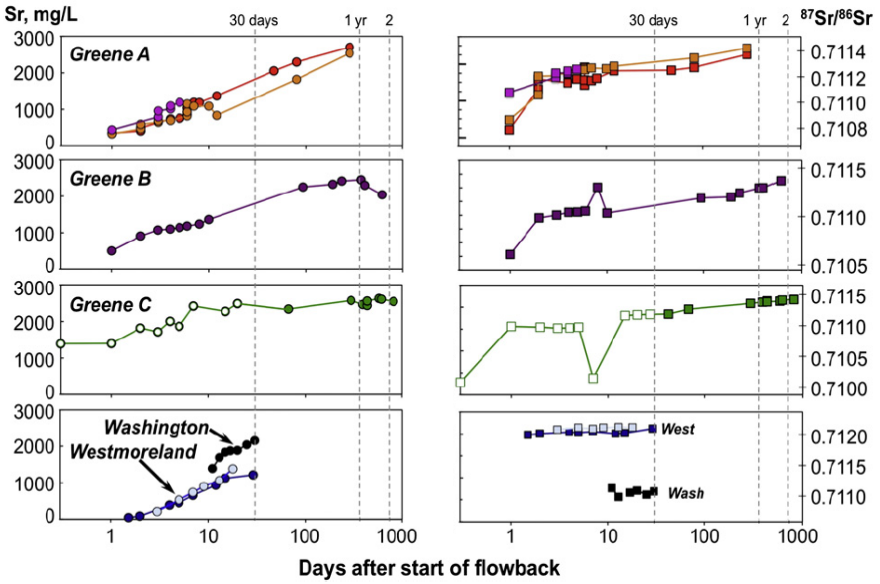

Figure 1-11. Results from Marcellus flowback samples by county showing an increase of Sr concentration and $^{87}Sr/^{86}Sr$ over time (from Capo et al., 2013).

1.7 Mixing Curve

Within the Bakken Formation in North Dakota, Peterman et al. (2012) studied Sr isotopes to determine if they could be used to detect small amounts of oil field brine in groundwater samples collected from wells and wetlands. A mixing curve was produced from their results (Fig. 1-12) demonstrating that predictable relationships can be used to detect whether even very small amounts of oil field brine have mixed with surface waters. An uncontaminated surface water sample composed of small concentrations of Sr will undergo a sudden and quick drop in the samples radiogenic signature by mixing in very small amounts (1%) of oil field brine composed of high concentrations of Sr. Any mixing between the oil field brine and surface waters will fall below the upper line in Fig. 1-12 (passing through 264J). As contamination concentrations increase, the sample's $^{87}Sr/^{86}Sr$ moves down along the curves towards the isotopic composition of the oil field brine. One advantage to using $^{87}Sr/^{86}Sr$ as a geochemical fingerprint is that $^{87}Sr/^{86}Sr$ will not change

due to evaporation. This is shown visually (Fig. 1-12) where evaporation will increase the concentration of Sr as water is removed, leaving behind Sr (proceeding along the x-axis), with its $^{87}Sr/^{86}Sr$ (y-axis) remaining the same.

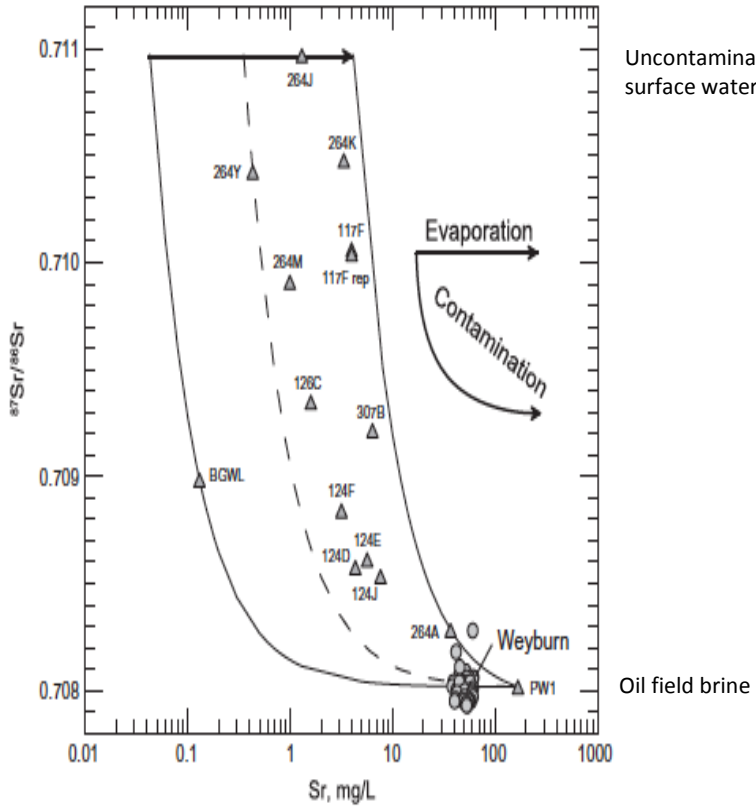

Figure 1-12. Evaporation-mixing model for Sr isotope variations in surface waters at differing oil field brine concentrations from Goose Lake. Triangles are sample sites. (From Peterman et al., 2012).

1.8 Hypothesis

In order to determine if $^{87}Sr/^{86}Sr$ can be used as fingerprint for the provenance of total dissolved solids (TDS) within the region overlying the Barnett Shale, I tested samples from different sources for Sr concentrations and ratios of $^{87}Sr/^{86}Sr$. I hypothesized that the aquifer water samples, flowback, and the sequential extractions from the Barnett Shale, will show unique Sr radiogenic values based on their source of Sr. This will be useful for determining if any mixing has occurred between fluids of differing provenance. I further hypothesized that the values of $^{87}Sr/^{86}Sr$ of the flowback sample and the H_2O sequential extraction of samples from a Barnett Shale core will most

resemble each other. This assumption is based on the water leachate being a reasonable approximation of hydraulic fracturing fluid interacting with shale and formation fluids (Stewart et al., 2015).

To help determine if an aquifer has been contaminated by flowback, mixing curves similar to that in Fig. 1-12 will be constructed between aquifer (low Sr concentration and $^{87}Sr/^{86}Sr$) and flowback (high Sr concentration and $^{87}Sr/^{86}Sr$) samples as end members. The curve reflects the varying proportion of the end members in a mixed fluid. A mixture will fall on the curve depending on the percentage of flowback relative to aquifer (uncontaminated water). It is evident from looking at the mixing curve (Fig. 1-12) that the $^{87}Sr/^{86}Sr$ of a mixture that begins as an uncontaminated aquifer will quickly increase by adding only minimal amounts of flowback (<1%). If a contaminated aquifer does not fall on this mixing curve then the source of Sr contamination is not from flowback.

Chapter 2

Study Site

2.1 Stratigraphy

The stratigraphic column (Fig. 2-1) displays a generalized view of the geologic formations in the study area and their age, relative thickness, lithology, and $^{87}Sr/^{86}Sr$ values. The formations that are of interest to the study are the Barnett Shale, the section from the Twin Mountain Formation up to the Paluxy Formation (Trinity aquifer host formations), and the Woodbine Formation (Woodbine aquifer host rock).

The Barnett Shale is of great economic importance (Loucks and Ruppel, 2007). It was deposited concurrently with the subsidence of the Ft. Worth Basin (Al Salem, 2014) during a marine transgression in the Late Mississippian (Abouelresh and Slatt, 2012). The thickness and lithology of the Barnett Shale vary spatially (Fig. 2-2) (Loucks and Ruppel, 2007). In the NE section of the study area, the Barnett Shale was divided into upper and lower subunits by the Forestburg Limestone, which pinches out to the SW (Fig. 2-3). The Forestburg Limestone was deposited during a large-scale marine transgression when the silicic input was low (Loucks and Ruppel, 2007).

The productive part of the Barnett Shale covers 12,950 km^2 underlying over 18 counties in the DFW Metroplex ("Barnett Shale Information," 2016) (Figure 1-1) and has been drilled disproportionately with horizontal wells.

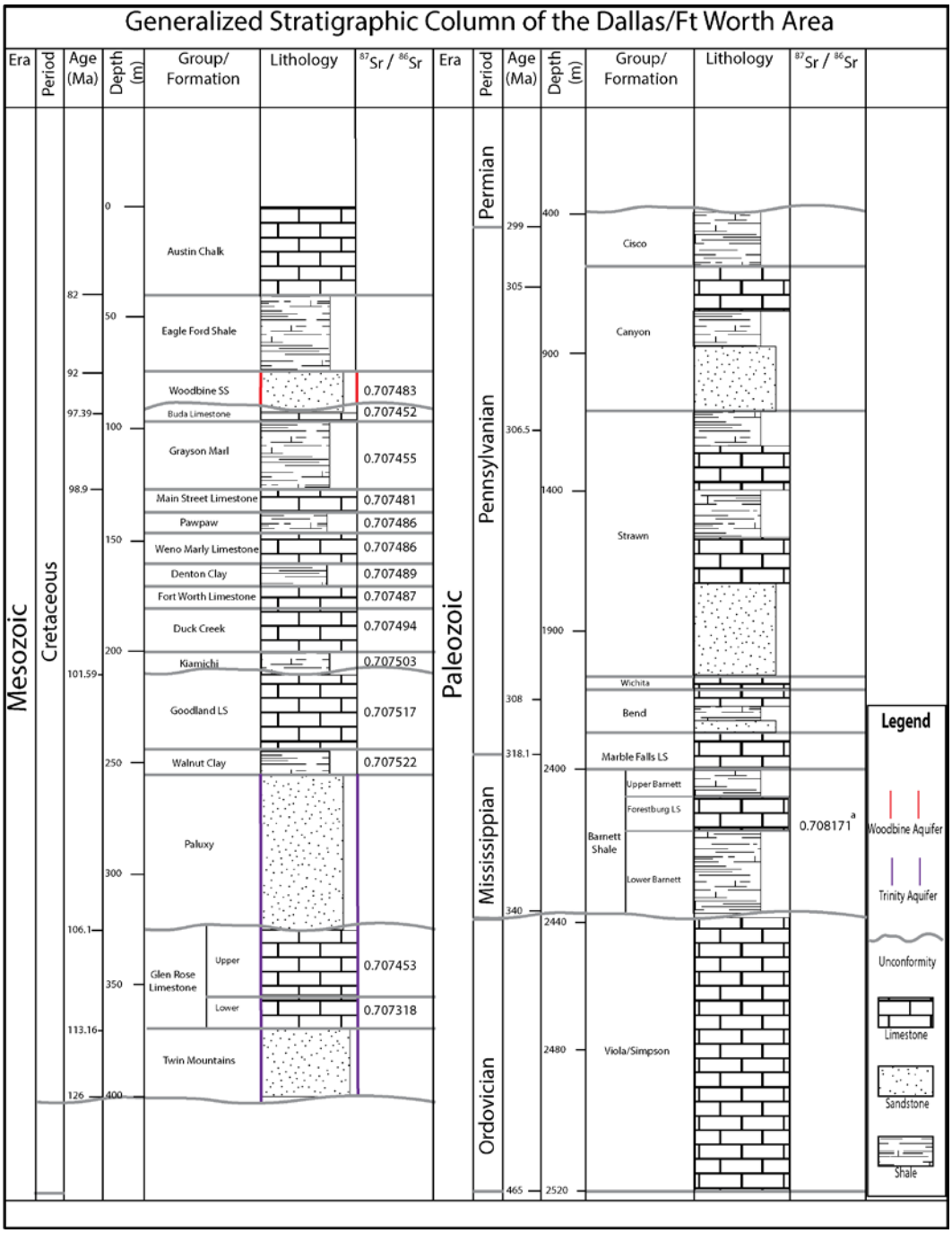

Figure 2-1. Generalized stratigraphic column of the study area. All $^{87}Sr/^{86}Sr$ values except "a" are from Denison et al. (2003). Reference "a" = Dennie (2010). Age, thickness, lithology are from Turner (1957); Denison et al. (2003); and Al Salem (2014).

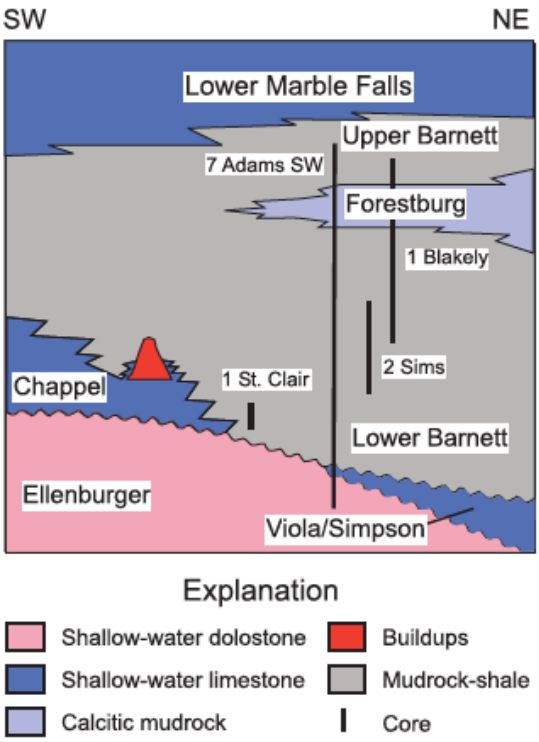

Figure 2-2. Generalized illustration of the change in stratigraphy within the DFW Metroplex (from Loucks and Ruppel, 2007).

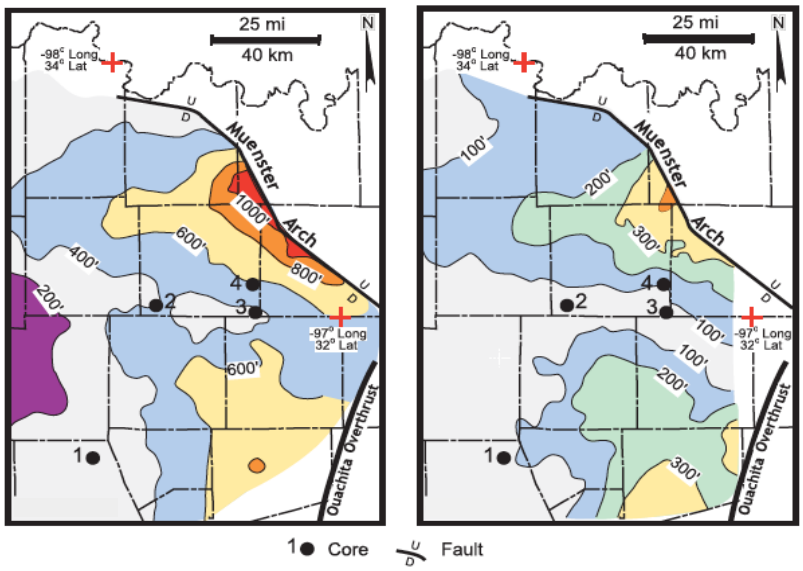

Figure 2-3. Isopach maps of the Barnett Shale (left panel) and Forestburg Limestone (right panel); Core 3 = Texas United Blakely #1 (from Loucks and Ruppel, 2007).

The Trinity aquifer (Fig. 2-4) stretches across the north central portion of Texas and is one of the most extensively used groundwater resources for drinking and agriculture in Texas ("Trinity Aquifer," 2016). Within the study area, the Trinity aquifer is situated within the Cretaceous Twin Mountains Formation, Glen Rose Limestone, and Paluxy Sandstone (Fig. 2-1) with most of the water resources being drawn from the Twin Mountains and Paluxy formations (Nordstrom, 1982). The productive part of the Trinity aquifer also varies in depth and can be found up to 1524 meters below the surface (Kelley et al., 2014). To the west, outside of the study area, the Glen Rose Limestone pinches out and the Twin Mountains and Paluxy formations converge to form the Antlers Formation. The host formations of the Trinity aquifer were deposited during a series of marine transgressions and regressions with fluvial depositional environments dominating the west side and a wave-dominated deltaic environment in the east side of the basin (Holland, 2011). The Twin Mountains Formation is primarily composed of sandstones (Hosston Sandstone, Hensel Sandstone) with minor interlayered carbonate and shale (Pearsall Formation, Sligo Limestone). The Glen Rose Formation is composed of limestone, marl, and shale and the Paluxy Formation is composed of fine-grained sandstone and shale (Chaudhuri and Ale, 2013). The formations that make up the Trinity aquifer influence the groundwater chemical composition as interaction between recharged meteoric waters react with the formations themselves causing mineral weathering and ion exchange.

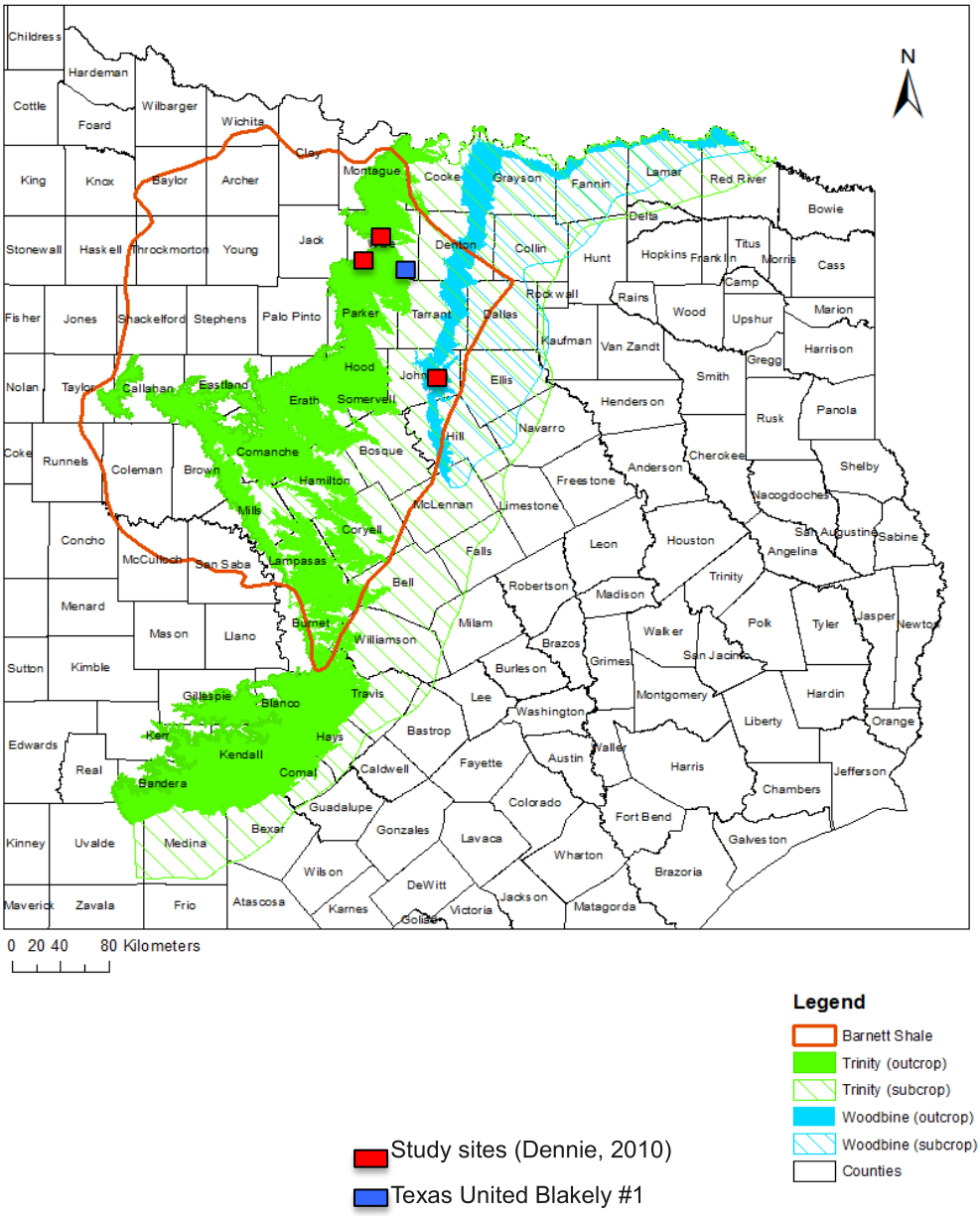

Figure 2-4. Map of study site displaying extent and relative locations of the Barnett Shale and Trinity/Woodbine aquifers. ("Shapefile of DFW Aquifers," 2015) ("Shapefile of Barnett Shale," 2015) (“Shapefile of Texas counties,” 2015).

The study area contains several smaller aquifers, including the Woodbine aquifer, which is located above the Trinity aquifer in the eastern portion of the study area

(Fig. 2-4). The Woodbine aquifer is located within the Cretaceous Woodbine Formation (Fig. 2-1), which is composed of medium- to coarse-grained sandstone with interbedded shale and lignite (Peckham et al., 1963). The depositional environment of the Woodbine Formation was similar to the formations of the Trinity aquifer, including both the fluvial and deltaic environments. The Woodbine Formation can also be found at various depths across the study site. The Woodbine Formation can be found in outcrop to the northwest, dipping to the southeast. The productive part of the formation varies depending on location and can be found over 450 meters below the surface (Kelley et al., 2014).

2.2 Geochemical Background

Groundwater within the Trinity and Woodbine aquifers has been analyzed previously for elemental concentrations. A pair of related studies conducted at different time periods (Table 2) collected and analyzed samples from drinking wells within 5 km of active hydraulic fracturing activities in the Barnett Shale and from drinking wells within the same area that were not near current extraction sites (Fontenot et al., 2013; Hildenbrand et al., 2015) (Table 2-1). Analyses were performed to detect amounts of TDS, arsenic (As), barium (Ba), and strontium (Sr) within the samples. The data were compared to a historical data set compiled from the Texas Water Development Board, which is composed of 330 private drinking well samples collected between 1989-1999 before hydraulic fracturing began in the Barnett Shale. TDS from both studies generally displayed results consistent with the historical data and is known to be naturally elevated in the area (Chaudhuri and Ale, 2013; Fontenot et al., 2013). As and Sr were elevated in the samples collected in 2011 compared to the historical data, then decreased from 2011 to 2013-2014. A potential explanation is the buildup of iron oxide rust or scale formations within water wells that were liberated through ground disturbances caused by drilling

activities releasing As and Sr ([From Groat and Grimshaw, 2006]; Fontenot et al., 2013). In turn, as drilling activity decreased from 2011 to 2013-2014 the subsequent drop in hydraulic fracturing activities caused a drop in the concentration of these elements leaching into the groundwater (Hildenbrand et al., 2015). While these studies provide insight into whether contamination events have occurred, they do not provide a method for determining the source of a potential contaminant. Measuring $^{87}Sr/^{86}Sr$ can potentially provide this information.

The $^{87}Sr/^{86}Sr$ of fossil fragments (oyster, pectin, echinoid) found in the Commanchean Series in north Texas and southern Oklahoma were used to help define the unaltered marine carbonate formations in the region (Denison, 2003; Fig. 2-1). Within the Barnett Shale, Dennie (2010) analyzed calcite and barite cements in rock cores from well sites across Wise and Johnson Counties (Fig. 1-8) to investigate the influence of externally derived fluids (diagenesis) on $^{87}Sr/^{86}Sr$ within the Barnett Shale. The wells were situated between the Muenster Arch and the Ouachita Thrust Belt running from the NW to the SE with the Wise County wells being most distal from the NE-SW trending Ouachita Thrust. The cements from Wise County displayed an average $^{87}Sr/^{86}Sr$ ratio of 0.708191 (n=10; range=0.708090-0.708430) with values relatively coeval with the value for seawater $^{87}Sr/^{86}Sr$ at this time (Denison et al., 1998). The cements from Johnson County displayed an average $^{87}Sr/^{86}Sr$ ratio of 0.709021 (n=7; range=0.708090-0.709940), much higher then the seawater curve (Denison et al., 1998). Dennie (2010) proposed that the higher $^{87}Sr/^{86}Sr$ values found in Johnson County (proximal to the Ouachita Thrust Belt) are due to increased amounts of externally derived fluids as a result of tectonic movement along the thrust belt.

Table 2-1. TDS and selected metal concentrations in well samples sourced from the Trinity and Woodbine aquifers located within active and non-active fracturing sites.

Year	TDS ppm			Ba ppb			Sr ppm			As ppb		
	Mean	n	Range	Mean	n	Range	Mean	n	Range	Mean	n	Range
TWDB	670.3	344	129-3302	57.2	357	0.1-382.0	1.0	99	0.02-16.7	2.8	241	1.0-10.0
FA	585.1	91	200-1900	32.3	90	1.8-173.7	2.3	90	0.07-18.2	12.6	90	2.2-161.2
HA	598.5	500	68.5-1891.5	141.9	487	10.2-4380.8	1.1	358	0.1-9.0	1.3	483	0.001-114.4
FNA	525.0	9	400-600	27.0	9	12.0-46.5	3.0	9	0.9-7.6	5.4	9	4.7-6.6
HNA	948.5	50	275.6-3328	68.1	48	12.2-296.9	0.4	35	0.1-4.7	2.4	49	0.01-21.3

TWDB= Texas Water Development Board 1989-1999; FA= 2011 Fontenot active and FNA= 2011 Fontenot non-active from Fontenot et al. (2013). HA= 2013-2014 Hildenbrand active and HNA= 2013-2014 Hildenbrand non-active from Hildenbrand et al. (2015).

Chapter 3

Methods

3.1 Sample Collection

Flowback sample

A flowback sample from hydraulic fracturing activities was obtained from Dr. Qinhong Hu in the Department of Earth and Environmental Sciences at The University of Texas at Arlington. The flowback sample was acquired from hydraulic fracturing activities in the Barnett Shale by a treatment remediation firm who sought elemental concentrations of the flowback. The sample was previously analyzed for elemental concentrations on an inductively coupled plasma mass spectrometer (ICP-MS) in Dr. Hu's lab. Permission was granted to do additional analysis on the sample for this project, specifically analysis of Sr isotopes.

Aquifer Samples

Aquifer samples (n = 5) were provided by Drs. Kevin Schug and Doug Carlton in the Department of Chemistry and Biochemistry at The University of Texas at Arlington. Five samples (Table 3-1) were pulled from their sample set (n=550), which was collected between 2013-2014 from private drinking wells (depth=10-1200 m) tapping either the Trinity and Woodbine aquifers in the counties surrounding the Ft. Worth area. All wells were located less than 1.5 km from hydraulic fracturing activities (Hildenbrand et al., 2015). Samples were collected as close to the wellhead as possible, bypassing filters or treatment systems (Fontenot et al., 2013). A YSI Professional Plus multi-parametric probe was used by Hildenbrand et al. (2015) to measure temperature, dissolved oxygen, and conductivity which were then used to calculate TDS (Table 2-1). Salinity, pH, and

oxidation-reduction potential of the samples was also measured using a YSI Professional Plus multi-parametric probe. Wells were purged until measurements stabilized for each parameter to ensure proper characterization of the aquifer's fresh water reserve. Samples were collected in photo-resistant HDPE bottles with no headspace. The samples were filtered and preserved to a pH less then two with nitric acid and then stored at 4° C (Hildenbrand et al., 2015).

Table 3-1 List of private well samples with aquifer source and distance from active hydraulic fracturing activities collected by Hildenbrand et al. (2015).

Sample #	Aquifer	Distance (km)	Depth (m)
98	Woodbine	1.22	259.1
117	Trinity	0.70	86.9
182	Trinity	0.92	30.5
246	Woodbine	0.44	67.1
422	Woodbine	1.03	477.1

Organic compounds and elemental concentrations (Table 2-1) were determined using gas chromatography-mass spectrometry (GC-MS), headspace-gas chromatography (HS-GC), inductively coupled plasma - mass spetrometry and optical emission spectroscopy (ICP-MS and ICP-OES), and ion chromatography (IC) (Hildenbrand et al., 2015).

Barnett Shale Core Samples

Powdered samples (Fig 3-1) (~0.5 g; n=3) from the Barnett Shale (Texas United Blakely #1, Wise County Texas (location shown in Fig 2-4) were obtained from Dr. Qinhong Hu in the Department of Earth and Environmental Sciences at The University of Texas at Arlington. Sample 1 was a composite from various depths sourced from the Forestburg Limestone and Lower Barnett Shale (depth = 2169-2184 m) (Loucks and

Ruppel, 2007). A second composite sample from Blakely #1 was sourced from the Lower Barnett Shale (depth = 2184-2202 m) (Loucks and Ruppel, 2007). Two sub-samples were taken from the Lower Barnett sample, which were prepared and analyzed as duplicates (samples 2A and 2B accordingly). Parts of the cores were cut into chips and then pulverized to a powder <75 μm (Fig 3-1).

a) b)

Figure 3-1 Powdered Barnett Shale core samples (filter paper size = 7.62 cm x 7.62 cm) a = Sample 1 (depth 2169-2184 m); b = Sample 2 (depth 2184-2202 m).

3.2 Procedures

Sequential Extractions

The Barnett Shale powders (approximately 0.5 g each) and a method blank were subjected to a series of sequential extractions in order to target different soluble fractions and mineral phases within the samples following Stewart et al. (2015). Each sample (n = 3) was collected and placed in a pre-weighed, acid washed 50 mL centrifuge tube.

The first sequential extraction used ultrapure water (H_2O) to target soluble salts and evaporated pore waters. It is anticipated that the H_2O extraction will most resemble the flowback sample compositionally and isotopically ($^{87}Sr/^{86}Sr$) since the water leachate is thought to be a reasonable approximation of hydraulic fracturing fluid interacting with shale and formation fluids (Stewart et al., 2015). 30 mL of ultrapure water was added to each centrifuge tube, shaken overnight and then centrifuged. The leachant was then poured into a syringe and filtered to <0.45 µL into pre-weighed, acid washed polypropylene bottles. 20 mL of ultrapure water was then added to each drained centrifuge tube, which was briefly shaken, centrifuged and filtered into each polypropylene bottle. A 3 mL aliquot was taken for pH analysis from each bottle. The pH was then measured using a YSI 1007-1 pH/Temp Probe. A second 3 mL aliquot was taken for anion analysis from each bottle (not done in this study) and then the sample was reweighed and acidified with 1 mL concentrated ultrapure nitric acid.

The second extraction targeted exchangeable cations bound to clays and used 1N ammonium acetate (AA) buffered to pH 8 with ammonium hydroxide. 30 mL of buffered AA was added to each centrifuge tube, which was shaken overnight and centrifuged briefly. The leachant was then poured into a syringe and filtered to <0.45 µL into pre-weighed, acid washed polypropylene bottles and weighed again. 20 mL of AA was added to each drained centrifuge tube, which was then briefly shaken, centrifuged and filtered into each bottle. The sample was then dried down and brought back up in 30 mL 2% HNO_3 for geochemical analysis. The same procedure followed for the AA leach was then performed on the samples in the centrifuge tubes a third time using 8% ultrapure acetic acid (Ac) to target carbonate minerals and a fourth time using 0.1N hydrochloric acid (HCl) to target other acid soluble fractions.

The 2% HNO_3 was created in a 500 mL volumetric flask using 10 mL of Fisher Scientific trace metal grade nitric acid mixed with 490 mL of ultrapure water.

Elemental Analysis

For consistency, elemental concentrations of the leach samples were analyzed twice on the Shimadzu ICPE-9000 Multi-type ICP Emission Spectrometer at the Shimadzu Center for Advanced Analytical Chemistry at The University of Texas at Arlington. Standards were created as listed in Table 3-2, which were diluted to desired concentrations with 2% HNO_3, made using ultrapure water and trace metal grade acid. Standards for both runs were based on expected concentrations (Tables 3-3, 3-4, 3-5) derived from prior analysis performed in the Marcellus Shale (Stewart et al., 2015). This was done with the knowledge that the Marcellus Shale is not an analog of the Barnett Shale (Hildenbrand et al., 2015; Stewart et al., 2015) but it served as a good starting point. Standard concentrations were modified for Run 2 based on the results of the Run 1 samples.

Table 3-2 List of standards used for analysis on ICP-OES.

Element	Manufacturer	ppm (mg/L)	Matrix
Barium	Ricca Chemical Co.	1000 +/- 5 mg/L	3% Nitric
Calcium	Ricca Chemical Co	1000 +/- 3 mg/L	3% Nitric
Iron	SPEX CertiPrep	100 +/- 0.5 mg/L	5% Nitric
Magnesium	Ricca Chemical Co	1000 +/- 3 mg/L	3% Nitric
Potassium	SPEX CertiPrep	1000 +/- 5 mg/L	2% Nitric
Sodium	SPEX CertiPrep	1000 +/- 5 mg/L	2% Nitric
Strontium	Ricca Chemical Co	1000 +/- 5 mg/L	3% Nitric

Table 3-3 Amount of elemental standards used to create high standard (in 50 mL volumetric flask) for Runs 1 and 2 on ICP-OES.

Element	Run 1		Run 2	
	Desired ppm	µL of Std.	Desired ppm	µL of Std.
Barium	10	500		
Calcium	200	10,000	120	6000
Iron*			50	2000
Magnesium	40	2000	10	500
Potassium			10	500
Sodium			10	500
Strontium	5	250	50	2500

* Iron standard diluted in small vial

Table 3-4 Amount of elemental standards used to create medium standard (in 50 mL volumetric flask) for Runs 1 and 2 on ICP-OES.

Element	Run 1		Run 2	
	Desired ppm	µL of Std.	Desired ppm	µL of Std.
Barium	1	50		
Calcium	20	1000	60	3000
Iron			5	2500
Magnesium	2	100	1	50
Potassium			1	50
Sodium			1	50
Strontium	1	50	1	50

Table 3-5 Amount of elemental standards used to create low standard for Runs 1 and 2 on ICP-OES.

Element	Run 1 (in 100 mL flask)		Run 2 (in 500 mL flask)	
	Desired ppm	µL of Std.	Desired ppm	µL of Std.
Barium	0.1	10		
Calcium	2	200	8	4000
Iron			0.1	500
Magnesium	0.2	20	0.1	50
Potassium			0.1	50
Sodium			0.1	50
Strontium	0.1	10	0.1	50

Samples were run undiluted and with various samples at a 10% dilution, which were created due to expected high concentrations of calcium in the Ac leach. For Run 1, the Ac leach was diluted to 10%. Due to higher then expected concentration results from Run 1, 10% dilutions were performed on the Ac, AA, and HCl leaches for Run 2. All samples for both runs resided in a matrix of 2% trace metal nitric acid. Run 2 also included additional analyses of iron, sodium, and potassium on the leaches. Wavelengths used on the ICP-OES for both runs are listed by element in Table 3-6. Precision (Table 3-6) for run 1 is reported as RSD on the low standard (n=3) and run 2 on the medium standard (n=2).

Table 3-6 Wavelengths used and precision for Runs 1 and 2 on ICP-OES.

Element	Run 1	RSD	Run 2	RSD
Barium	455.403	1.1%		
Calcium	183.801	6.0%	317.933	1.3%
Iron			238.204	1.3%
Magnesium	383.826	13.1%	280.270	0.0%
Potassium			766.490	2.8%
Sodium			589.592	1.3%
Strontium	216.596	5.2%	216.596	2.7%

Extraction Chromatography

A column procedure modified from Scher et al. (2014) was used to purify the samples using Eichrom Sr Spec resin in the Clean Lab at the University of Texas at Arlington in preparation for Sr isotope analysis on the thermal ionization mass spectrometer (TIMS) at The University of Texas at Arlington and a multi-collector inductively coupled plasma mass spectrometer (MC-ICPMS) at The University of South Carolina. In preparation for the Sr separation, a sample volume containing 1 µg of Sr was dried down, reconstituted in 100 µL Fisher Scientific ultrapure 8M nitric acid and then

placed in an ultrasonic bath to completely dissolve the sample. 125 µL columns were filled with approximately 0.125 mL of Eichrom® Sr Spec resin in 0.005 M HNO_3 (Fig. 3-2). The columns were washed with 600 µL of 0.005 M HNO_3 and then conditioned with 200 µL of 8N HNO_3. Each reconstituted sample was loaded onto a separate column and washed with 2 mL of 8M HNO_3. Finally, the Sr within the sample was eluted into acid washed Teflon vials by adding 1 mL of 0.005 M HNO_3.

Figure 3-2 125 µL Teflon column, photo taken in UTA Clean Lab by the author.

In order to determine whether the Sr column method was purifying and capturing the Sr loaded onto the column (prior to its use with samples) a test run of the elution process was performed and Sr concentrations confirmed on the ICP-OES. The goal of the elution procedure is to separate Sr from other cations in solution. The results (Fig. 3-3) of the test elution showed the method was successful in capturing Sr within the cut defined in the method described above and illustrated in Fig. 3-3.

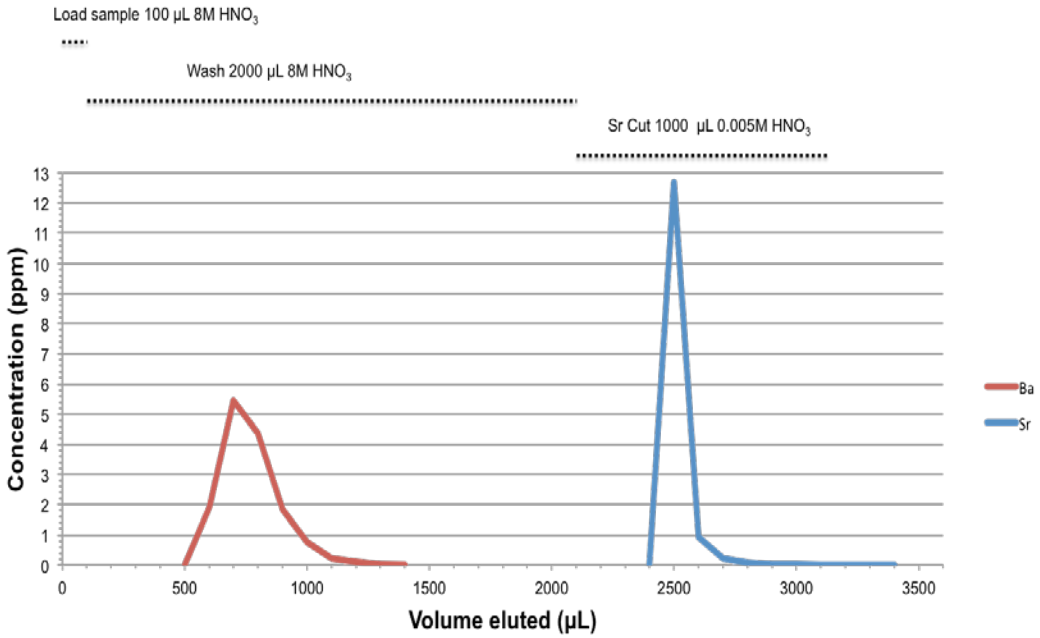

Figure 3-3 Results of extraction chromatography run performed on ICP-OES at UTA showing capture results of Ba and Sr, 2/25/15.

Thermal Ionization Mass Spectrometer (TIMS)

The VG Sector Thermal Ionization Mass Spectrometer at the Department of Earth and Environmental Sciences at The University of Texas at Arlington was used to measure $^{87}Sr/^{86}Sr$ of the flowback and aquifer samples, along with the Sr standard SRM 987. Analysis of SRM 987 (n = 1) gave a value of 0.710268 +/- 0.000034 (2SD) which is within error the same as the accepted value of 0.710248 (McArthur, 1994). 1 µg of Sr from each sample was loaded on to tantalum filaments for analysis. Measured $^{87}Sr/^{86}Sr$ ratios were normalized to $^{86}Sr/^{88}Sr = 0.1194$. Uncertainties on the samples were less then five in the in the fifth decimal place (2SD). Reported $^{87}Sr/^{86}Sr$ values have been normalized to SRM 987 $^{87}Sr/^{86}Sr = 0.710248$ (McArthur, 1994).

Multicollector Inductively Coupled Plasma Mass Spectrometer (MC-ICPMS)

The $^{87}Sr/^{86}Sr$ of the leachate samples were measured on a Neptune Plus Multicollector Inductively Coupled Plasma Mass Spectrometer at the Center for Elemental Mass Spectrometry at the University of South Carolina following the method of Widanagamage et al. (2014). The operating conditions were adjusted to optimize the signal intensity on mass 86. Masses 82, 83, 84, 85, 86, 87, 88, 90, and 91 were collected by static multi-collection. Samples were run with intensities of ~2 V on mass 86. Measured $^{87}Sr/^{86}Sr$ Sr ratios were normalized to $^{86}Sr/^{88}Sr$ =0.1194 (Widanagamage et al., 2014). Two analyses were performed (Tables 3-7 and 3-8) on the leachate samples. Analysis of SRM 987 for run 1 (n=13) gave a value of 0.710306 +/- 0.000012 (2SD). Analysis of SRM 987 for run 2 (n=6) gave a value of 0.710312 +/- 0.000005 (2SD). Reported $^{87}Sr/^{86}Sr$ values have been normalized to SRM 987 $^{87}Sr/^{86}Sr$ = 0.710248 (McArthur, 1994).

Table 3-7 Leachates analyzed and analysis of SRM 987 for run 1 on MC-ICPMS

	Leachate	SRM 987 (n=13)	
Sample 1	HCl		
Sample 2A	AA Ac	0.710306	0.000012
Sample 2B	Ac		

Table 3-8 Leachates analyzed and analysis of SRM 987 for run 2 on MC-ICPMS

	Leachate	SRM 987 (n=6)	
Sample 1	H_2O		
	AA		
	Ac		
Sample 2A	H_2O	0.710312	+/- 0.000005
	HCl		
Sample 2B	H_2O		
	AA		
	HCl		

Chapter 4

Results

4.1 Sequential Extractions

Geochemistry

Analyzed elements (Table 4-1) from the sequential extractions show varying geochemical affinities by leaching solution. Within the water-soluble phase (H_2O), Na (Fig. 4-1a) and K (Fig. 4-1b) were leached. Na was preferrentially leached in this phase (70-72% of total Na leached) with K showing considerable concentrations (20-24% of total K leached) and some Sr (Fig. 4-1d) contributed (10-12% of total Sr leached). The ammonium acetate (AA) phase leached elements from exchangeable cation sites. Ba (70-75% of total Ba leached; Fig.4-1c) and K (38-40% of total K leached; Fig. 4-1b) were preferentially leached in this phase. In addtion, the AA phase contributed significant concentrations of Sr (31-34% of total Sr leached; Fig. 4-1d) and some Ca (Fig. 4-1e). The carbonate phases (Ac leachate) preferentially extracted Ca (66-68% of total Ca leached; Fig. 4-1e) and Sr (40-43% of total Sr leached; Fig. 4-1d). Fe and Mg were also present in the Ac leachate. Mg (48-49% of total Mg leached; Fig. 4-1f) and Fe (53-55% of total Fe leached; Fig. 4-1g) were, however, preferentially extracted from the HCl leach (Table 4-1). K was also found in HCl leach in significant amounts (27-30% of total K leached; Fig. 4-1b).

Table 4-1 Element concentrations in leachates of Barnett Shale core cuttings. Concentrations are in µg/g of the original collected sample.

	Leachate	Ca	Ba	Mg	Sr	K	Fe	Na
Sample 1	H_2O	652	0.8	106	61	113	<DL	686
	AA	**25,540**	50.7	555	160	182	<DL	77
	Ac	**101,100**	7.0	**4600**	222	51	1992	119
	HCl	**22,270**	8.6	**5140**	67	128	2257	79
Sample 2A	H_2O	495	0.6	96	53	97	<DL	690
	AA	**23,290**	41.2	547	179	192	<DL	102
	Ac	**85,030**	8.1	**4090**	215	45	2398	108
	HCl	**18,000**	8.6	**4430**	78	141	2817	86
Sample 2B (duplicate)	H_2O	570	0.4	100	55	112	<DL	713
	AA	**24,210**	42.2	551	183	186	<DL	74
	Ac	**84,220**	7.1	**4120**	214	45	2406	107
	HCl	**17,880**	8.6	**4410**	81	145	2892	91

<DL = below detection limit; **bold** = Results calculated from analysis on 10% dilutions of leached sample.

a)

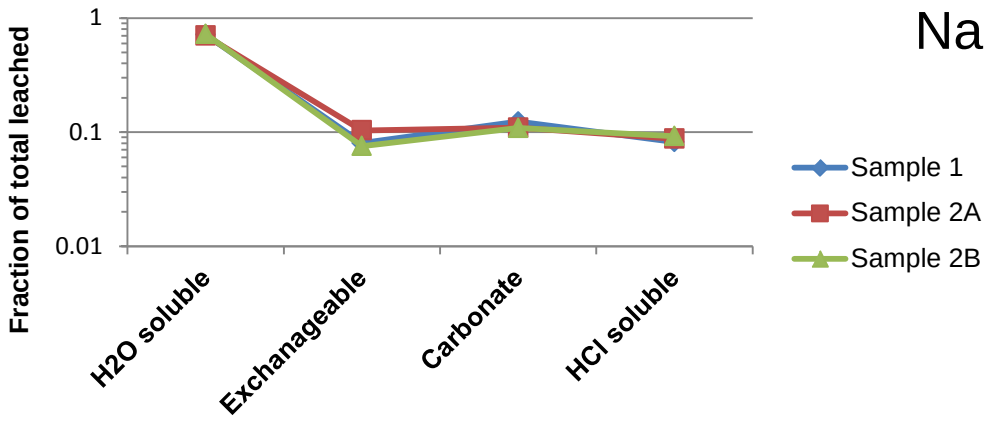
Na
Fraction of total leached
1
0.1
0.01
H2O soluble
Exchanageable
Carbonate
HCl soluble
Sample 1
Sample 2A
Sample 2B

b)

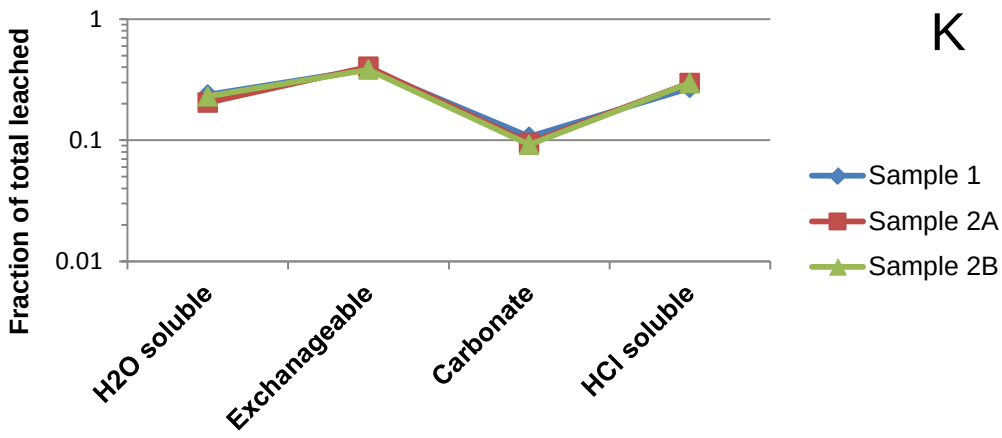
K
Fraction of total leached
1
0.1
0.01
H2O soluble
Exchanageable
Carbonate
HCl soluble
Sample 1
Sample 2A
Sample 2B

c)

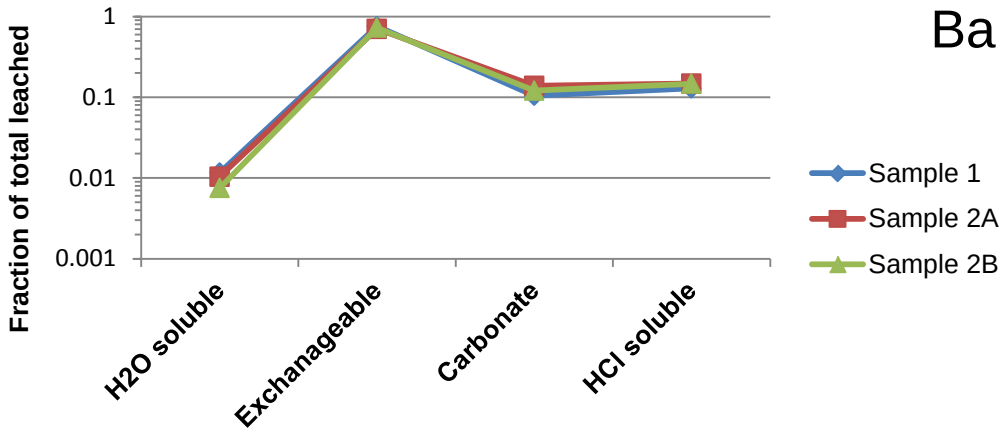
Ba
Fraction of total leached
1
0.1
0.01
0.001
H2O soluble
Exchanageable
Carbonate
HCl soluble
Sample 1
Sample 2A
Sample 2B

d)

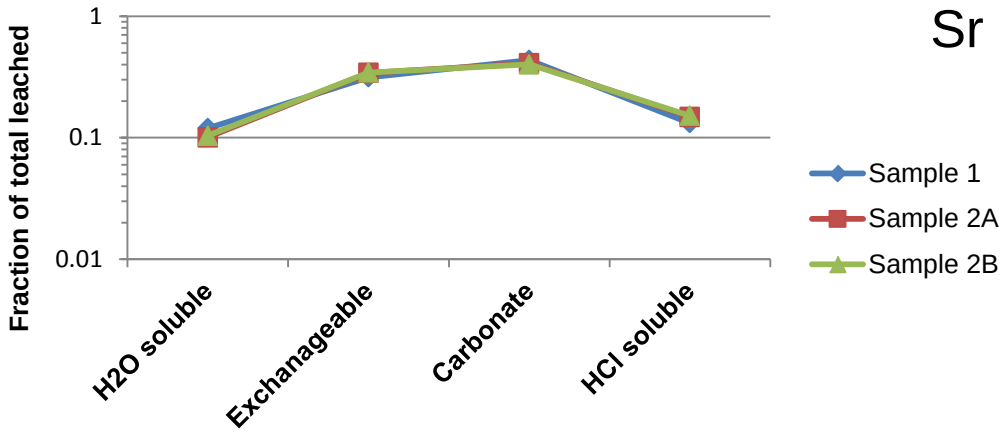
Sr
Fraction of total leached
1
0.1
0.01
H2O soluble
Exchanageable
Carbonate
HCl soluble
Sample 1
Sample 2A
Sample 2B

e)

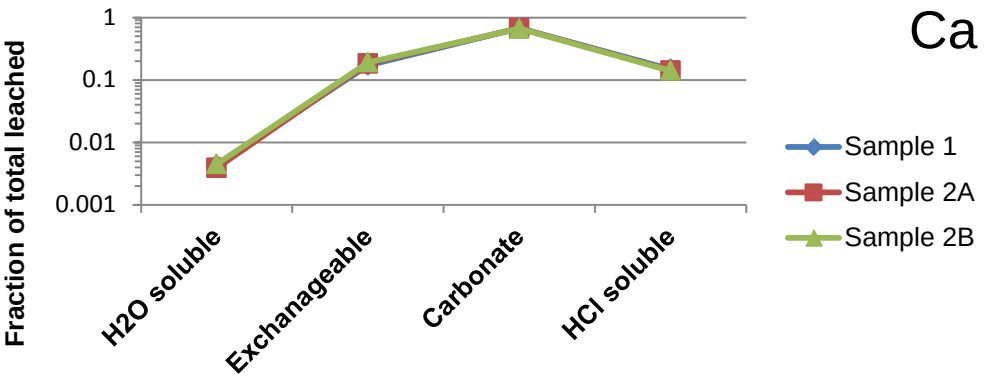
Ca
Fraction of total leached
1
0.1
0.01
0.001
H2O soluble
Exchanageable
Carbonate
HCl soluble
Sample 1
Sample 2A
Sample 2B

f)

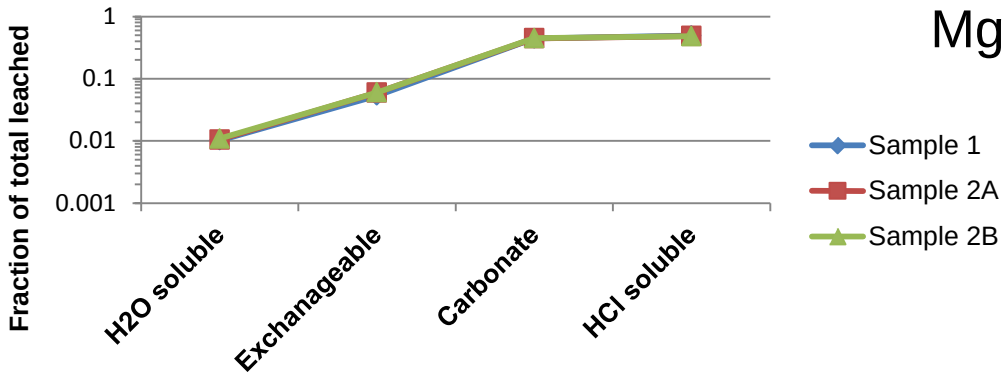
Mg
Fraction of total leached
1
0.1
0.01
0.001
H2O soluble
Exchanageable
Carbonate
HCl soluble
Sample 1
Sample 2A
Sample 2B

g)

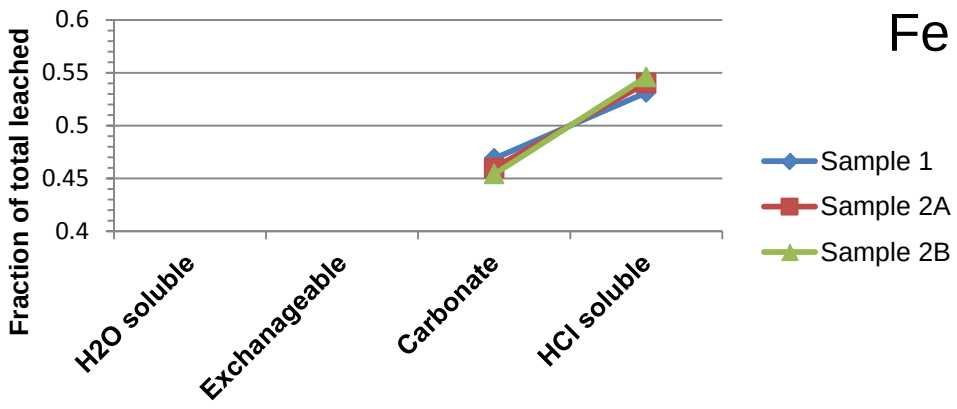

Figure 4-1 Fractions of Na (a), K (b), Ba (c), Sr (d), Ca (e), Mg (f), and Fe (g) leached by each sequential extraction. Order of the sequential extractions proceeds from left to right.

The total CO_3 weight percent for each sample (Table 4-2) was calculated from the total amount of Ca, Fe, and Mg (in µg) per g of each sample that was recovered from the acetic acid leachate (Table 4-1). To perform this calculation, Ca (in µg) was converted to moles of Ca (total Ca µg/40.08). This gives total moles of $CaCO_3$ within the acetic acid leachate (1 mol of Ca equals 1 mol $CaCO_3$). Moles of $CaCO_3$ were then converted to µg (moles of $CaCO_3$*100.09) to determine the total amount of $CaCO_3$ leached in each sample. This same procedure was used to calculate $MgCO_3$ and $FeCO_3$ substituting the proper weights for each element.

Table 4-2 Calculated total carbonate wt. % from acetic acid leach by sample

Sample 1	27.26%
Sample 2A	23.15%
Sample 2B	22.96%

Sr Isotopes

The $^{87}Sr/^{86}Sr$ of the samples (Table 4-3) show distinct trends with a couple inconsistencies. The $^{87}Sr/^{86}Sr$ of the acetic acid leaches were within error the same and consistently the lowest reported values (0.708232-0.708267; range=0.000035)). The H_2O leaches were nearly the same and consistently the second highest reported value for each sample (0.708889-0.708932; range=0.000043). The range of values measured for all samples in the ammonium acetate (0.708595-0.709164; range=0.000224) and HCl (0.708359-0.709070; range=0.000352) leaches were much higher than the H_2O and acetic acid phases, resulting in differences in which leachate had the highest values for each sample and the duplicate. Sample 2 was processed twice with the H_2O and Ac leaches replicating well with the AA and HCl leaches not reproducing with the same consistency having a difference of greater than five in the fifth decimal place.

Table 4-3 $^{87}Sr/^{86}Sr$ of Barnett Shale core samples by sequential extraction.

	Leachate	$^{87}Sr/^{86}Sr$ +/- 2SD		pH
Sample 1	H_2O	0.708932	+/- 0.000007	8.89
	AA	0.708939	+/- 0.000008	
	Ac	0.708267	+/- 0.000010	
	HCl	0.708359	+/- 0.000015	
Sample 2A	H_2O	0.708889	+/- 0.000006	8.58
	AA	0.708595	+/- 0.000020	
	Ac	0.708232	+/- 0.000009	
	HCl	0.709070	+/- 0.000006	
Sample 2B	H_2O	0.708895	+/- 0.000007	8.96
	AA	0.709164	+/- 0.000006	
	Ac	0.708255	+/- 0.000019	
	HCl	0.708711	+/- 0.000015	

4.2 Aquifer Samples

Geochemistry

Elemental concentrations of the aquifer samples (Table 4-4 from Hildenbrand et al. (2015)) show no overt trends between concentrations, depth, and pH. Concentrations of each element across all samples vary widely but in general are below the EPA's Drinking Water Maximum Contaminant Levels (Environmental Protection Agency, 2016) for Ba (2 mg/L) and the EPA's National Secondary Drinking Water Regulations limit for Fe (0.3 mg/L) (Environmental Protection Agency, 2016). Additionally, most of the samples fall under the health reference limit for Sr (4.2 mg/L; Alfredo et al., 2014). Exceptions include BS 246, which has Fe concentrations significantly in excess of 0.3 mg/L and BS 182, which has Sr in excess 4.2 mg/L. The other major elements studied for this research (Na, Ca, K, and Mg) do not have maximum containment levels or health reference limits listed by the EPA.

Sr Isotopes

The ratio of $^{87}Sr/^{86}Sr$ for the aquifer samples (Table 4-4) fall within a range of 0.707777-0.708252 (range=0.000475)). No direct correlation of an aquifers ratio of $^{87}Sr/^{86}Sr$ exists with pH, aquifer sampled, depth of well, distance from fracking site, or elemental concentrations.

4.3 Flowback Sample

Geochemistry

Elemental concentrations in the flowback sample (Table 4-5) are all extremely high relative to the aquifer samples with Ba, Fe, and Sr all in excess of their resepective limits set forth by the EPA as discussed in section 4.2.

Sr Isotopes

The $^{87}Sr/^{86}Sr$ of the flowback sample (Table 4-5) was significantly higher then all of the sequential leachates for each samples and for all of the the aquifer samples.

Table 4-4 Elemental concentrations and $^{87}Sr/^{86}Sr$ of the aquifer (well) samples.

Sample	Depth (m)	pH	Sr	Ba	Fe	S	Br	Cl	$^{87}Sr/^{86}Sr$ +/- 2SD	
BS 98 W	259	9.22	<0.075	0.024	0.045	86.70	<0.075	16.17	0.708191	+/- 0.000041
BS 117 T	87	7.20	4.034	0.252	0.058	274.96	<0.075	9.16	0.707966	+/- 0.000039
BS 182 T	30	6.79	8.968	0.403	0.308	519.11	0.34	88.05	0.708252	+/- 0.000039
BS 246 W	67	7.04	2.339	0.228	9.605	241.19	<0.075	154.32	0.707777	+/- 0.000036
BS 422 W	476	8.49	1.470	0.054	0.160	360.08	0.28	33.69	0.708137	+/- 0.000046

Elemental concentrations in mg/L T=Trinity Aquifer; W= Woodbine Aquifer. Elemental concentrations, pH, and depths from Hildenbrand et al. (2015). Uncertainties on the samples were less then five in the in the fifth decimal place (2SD).

Table 4-5 Elemental concentrations and $^{87}Sr/^{86}Sr$ of the flowback sample.

Ca	Ba	Mg	Sr	K	Fe	Na	Br	$^{87}Sr/^{86}Sr$ +/- 2SD	
11,072	9.83	919	433	277	2.07	20,874	416	0.711487	+/- 0.000035

Chapter 5

Discussion

5.1 Carbonate Mineralogy in the Barnett Shale

Based on the assumption that Ca, Mg, and Fe extracted by the acetic acid leach are from carbonate minerals, Ca carbonate is the predominant mineral in all of the samples (Fig 5-1; Table 5-1). This is shown by the results of (Mg+Fe)/(Ca+Mg+Fe) being a relatively low number due to Ca being high in the deonminator of (Mg+Fe)/(Ca+Mg+Fe). A comparison can be made to prior research from Stewart et al. (2015) who analyzed sequential extractions from the Marcellus Shale Formation, Hamilton Group, and overlying/underlying formations. The results from the Barnett Shale conform to a power law generated by Stewart et al. (2015) which shows that as the amount of total calculated carbonate weight percent increases, the amount of Ca carbonate minerals increases, with an accompanying decrease in the amount of Fe-Mg carbonate minerals. The acetic acid leaches from the Barnett Shale show higher total calculated carbonate weight percent than the Marcellus Shale. Within the carbonate, the Barnett Shale contains higher amounts of Ca carbonate minerals (µg/g sampled) compared to the Marcellus Shale (Stewart et al., 2015), which suggests higher amounts of calcite within the Barnett Shale as compared to the Marcellus Shale. Within this study, Sample 1 contains higher amounts of total carbonate compared to the duplicate Sample 2. This is most likely due to Sample 1 (depth = 2169-2184 m) being solely sourced from the Forestburg Limestone section of the Barnett Shale, whereas Sample 2A/2B (depth = 2184-2202 m) is a combination of the Forestburg Limestone and the Lower Barnett Shale (Fig. 5-2).

The HCl leaches from the Barnett Shale core samples (Table 5-1) contain higher ratios of (Mg+Fe)/(Mg+Fe+Ca) respresenting less soluble Fe-Mg carbonates such as dolomite ($CaMg(CO_3)_2$), siderite ($FeCO_3$), and ankerite ($CaFe(CO_3)_2$) which are common in the Barnett Shale (Dennie, 2010). The existence of these minerals provides further evidence that diagenesis has occurred within the Barnett Shale which explains why the $^{87}Sr/^{86}Sr$ within the acetic acid leach does not match expected $^{87}Sr/^{86}Sr$ from the Mississippian.

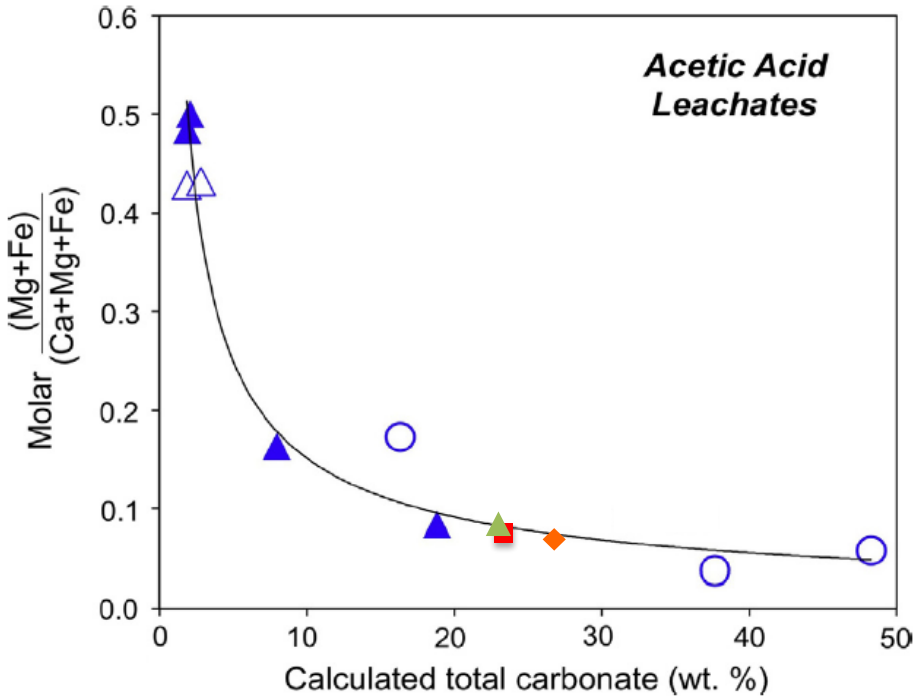

Fig. 5-1 Comparison of molar (Fe+Mg)/(Fe+Mg+Ca) of leached samples from acetic acid leachate versus total carbonate weight % of the Barnett Shale with prior research by Stewart et al. (2015). Results from Stewart et al. (2015) include: filled blue triangles=Marcellus Shale; open blue triangles=Hamiltion Group (limestones); open blue circles=overlying and underlying sandstones and limestones. Results from this study include: orange diamond=Sample 1; red square=Sample 2A; green triangle=Sample 2B. (Modified from Stewart et al., 2015).

Table 5-1 Molar (Mg+Fe)/(Mg+Fe+Ca) of Ac and HCl leach

	(Mg+Fe)/(Mg+Fe+Ca)	
	Ac leach	HCl leach
Sample 1	0.0818	0.3119
Sample 2A	0.0905	0.3411
Sample 2B	0.0918	0.3432

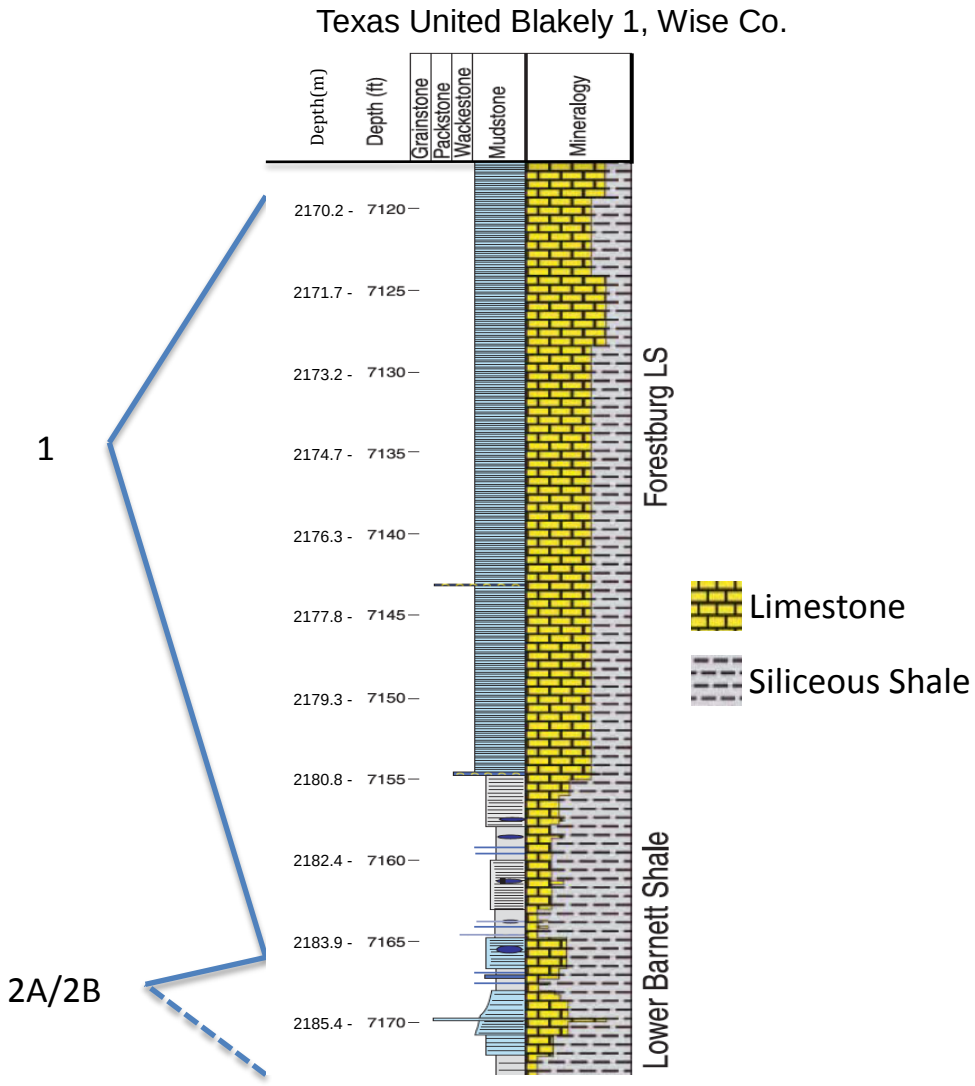

Fig 5-2 Minerology of Forestburg Limestone and Lower Barnett Shale sections within the Barnett Shale. 1= Sample 1 from this study; 2= Sub-samples 2A+2B taken from sample 2 for this study. Mineraology track based on XRD analysis and thin section examination (from Loucks and Ruppel, 2007).

5.2 Comparison of Barnett Shale Leachates to Flowback

Geochemistry

It was hypothesized that the H_2O leachates, which represent soluble salts are a reasonable approximation of fracturing fluid interacting with shale and formation fluids. This is important when considering the source of total dissolved solids in flowback water. Comparisons of the elemental molar ratios from the leachates (Sr/Ca, Na/Ca, Ba/Ca, K/Ca) (Fig. 5-3) show considerable overlap between the three core samples. When comparing the leachate molar ratios of Na/Ca, Ba/Ca, and Sr/Ca of all core samples against the flowback sample, it can be seen that the H_2O leach does provide the closest match, though the absolute concentrations themselves are significantly different. In contrast, the molar ratio of K/Ca of the flowback falls between the H_2O and the ammonium acetate leachate which represents exchangeable cations in clays (Fig. 5-2). This evidence indicates that while the H_2O leach is generally most similar to flowback, the total dissolved solids found in flowback are most likely not caused by the fracturing fluid interacting with solid components of the shale, but are instead coming from in situ formation fluids. This is corroborated by similar findings from Stewart et al. (2015) who postulated that total dissolved solids within the flowback are most likely being sourced from in situ formation fluids represented by salts measured in the H_2O leach of the core sample.

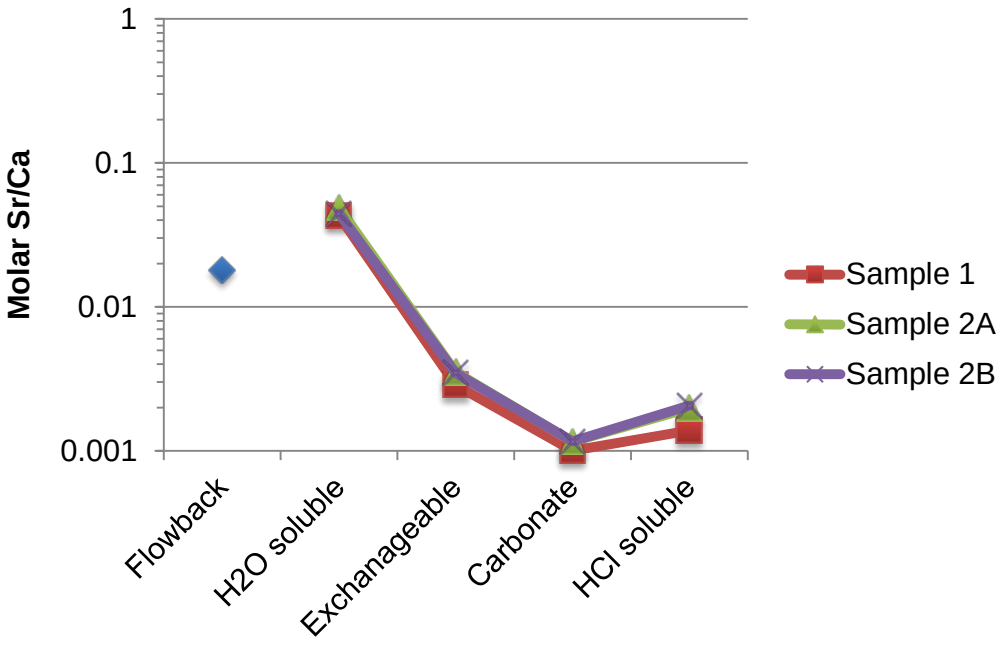
Molar Sr/Ca
1
0.1
0.01
0.001
Flowback
H2O soluble
Exchanageable
Carbonate
HCl soluble
Sample 1
Sample 2A
Sample 2B

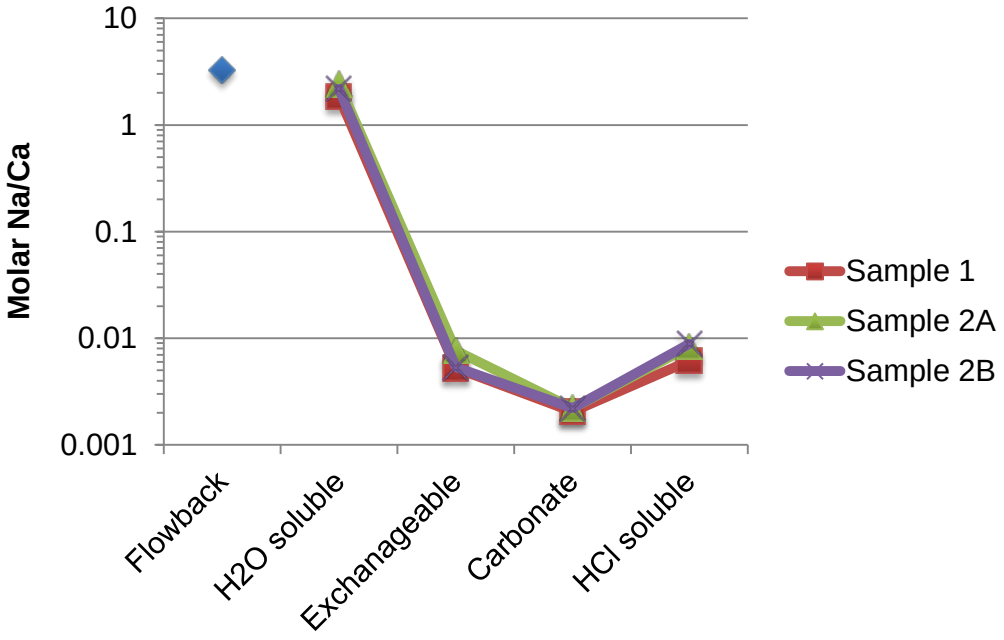
Molar Na/Ca
10
1
0.1
0.01
0.001
Flowback
H2O soluble
Exchanageable
Carbonate
HCl soluble
Sample 1
Sample 2A
Sample 2B

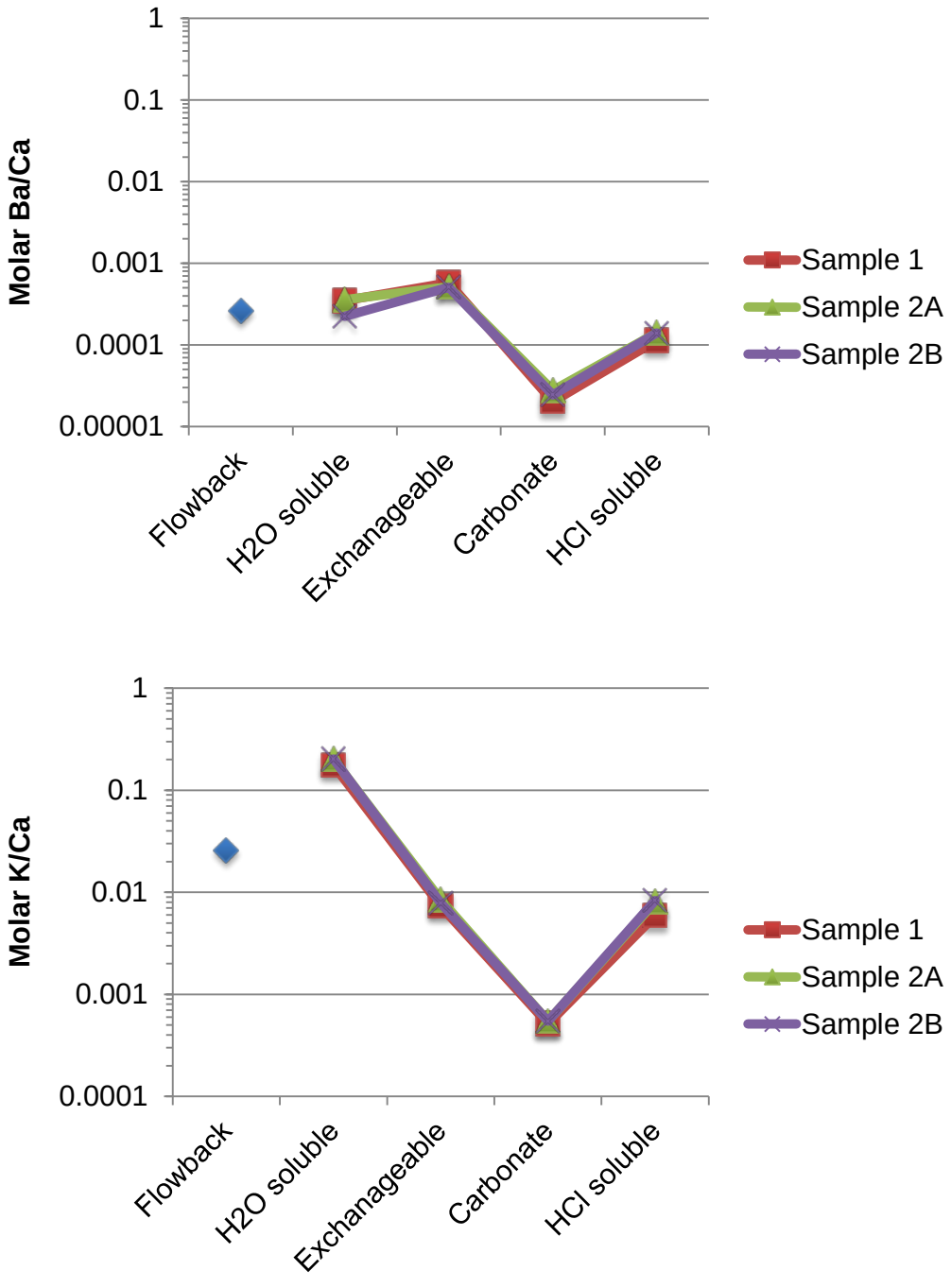

Fig. 5-3 Comparison of molar fractions by leachate for all core samples compared to the molar fractions of flowback sample.

Sr Isotopes

The Sr isotopes (Fig. 5-4) of the H_2O leachates were hypothesized to be a reasonable approximation of hydraulic fracturing fluid interacting with the Barnett Shale. The results of measurements on the H_2O leachates (0.708889-0.708932; n=3) and the flowback (0.711487, n=1) do not prove this hypothesis. The study was hindered by a limited sample set and uncertainties surrounding the origin and nature of the provided flowback sample. The regional location, timing of flowback sample collection, and the depth within the Barnett Shale that the flowback sample was collected are unknown. The regional location in particular is a critical component that must be known when comparing flowback to shale leachates. As shown by Capo et al. (2013) for the Marcellus Shale, the $^{87}Sr/^{86}Sr$ of flowback can vary widely by the regional location in which it was collected. Well sites whose locations varied by county produced highly variable $^{87}Sr/^{86}Sr$ results (0.710148-0.712117; n=32). The importance of regional sourcing of the samples is further corroborated by Dennie (2010). Regional variances of $^{87}Sr/^{86}Sr$ within his study showed that effects of diageneis (which will vary by regional location) via introduction of externally derived fluids will result in varying ratios of $^{87}Sr/^{86}Sr$ within carbonate cements found in the Barnett Shale (0.708090-0.709940; n=17). Pollastro et al. (2007) proposed that externally derived fluids within the Barnett Shale are introduced from the basement travelling into the Barnett Shale through a series of faults and fractures. The results from Dennie (2010) showed that $^{87}Sr/^{86}Sr$ values within the Barnett Shale increased with proximity to the Ouichita thrust belt where tectonic activity could have caused the introduction of externally derived fluids. Therefore, the location of sample collection is critical when comparing flowback to shale leachates.

The acetic acid leaches preferentially extract carbonate minerals from the shale. Comparing the results of the acetic leaches to expected marine carbonates from the

Mississippian (Fig. 5-4) show elevated $^{87}Sr/^{86}Sr$ within the acetic acid leach as compared to expected Mississippian carbonates. Again, the role of diagensis on the carbonate and the proposed introduction of externally derived fluids by Pollastro et al. (2007) can provide an explantion for this difference in $^{87}Sr/^{86}Sr$.

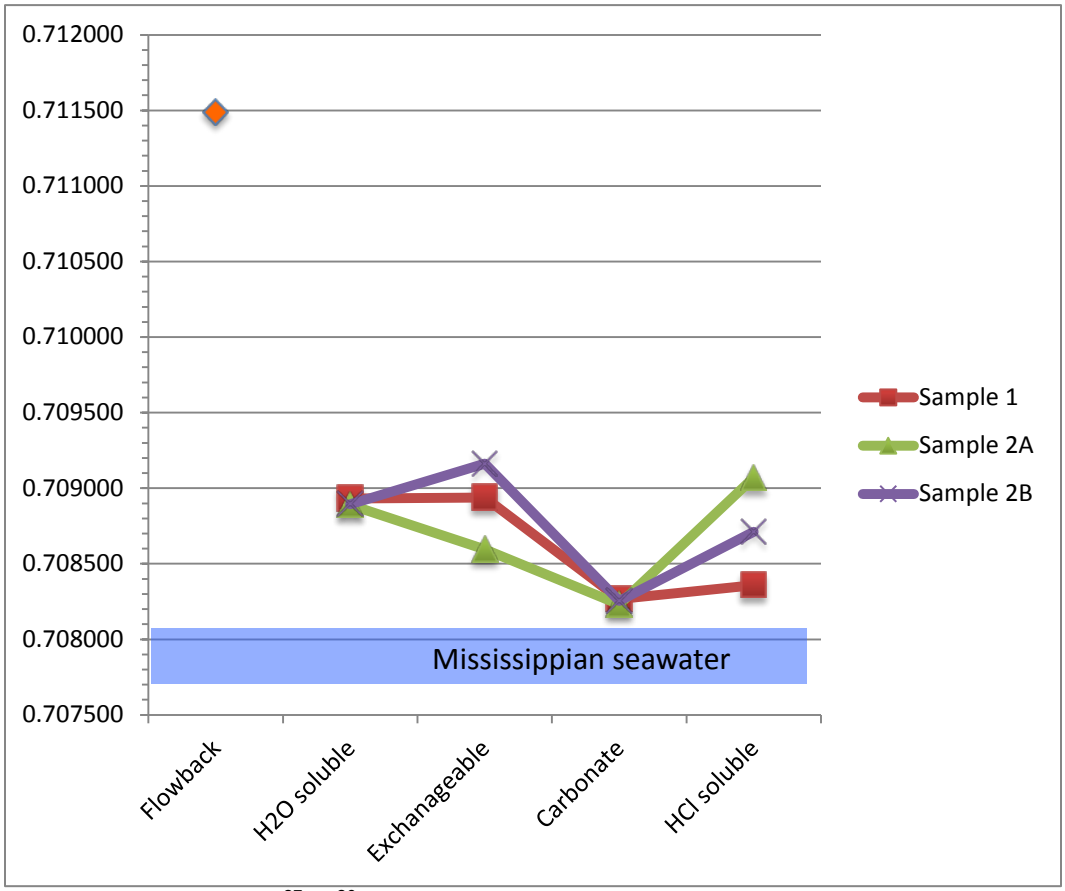

Fig. 5-4 Comparison of $^{87}Sr/^{86}Sr$ of the Barnet Shale leachates compared to the measured flowback sample. $^{87}Sr/^{86}Sr$ of Mississippian seawater from Denison et al. (1998).

5.3 Comparison of Aquifer Samples to Flowback

A theoretical mixing curve (Fig. 5-5) of a contaminant (PFW) with "uncontaminated" aquifer samples can be used to show the effect on $^{87}Sr/^{86}Sr$ by mixing of the end members. The flowback sample (n=1) for the study contains high

concentrations of Sr (433 mg/L) and high $^{87}Sr/^{86}Sr$ (0.711487). Aquifer samples (n=5) for the study contain relatively low concentrations of Sr (<0.075 to 8.968 mg/L) and $^{87}Sr/^{86}Sr$ ranging from 0.707777 to 0.708252.

As the mixing curve clearly demonstrates, contamination of an aquifer containing relatively little Sr is readily apparent. This is due to the small amounts of a highly concentrated Sr sample needed to alter its radiogenic Sr isotopic signature. The use of a mixing curve can then help to infer the source of the Sr contaminant by comparing the $^{87}Sr/^{86}Sr$ and Sr concentration of a sample between two end-members. If it falls on the mixing line, then the amount of the contaminant can be determined. If a "contaminated" aquifer sample, does not fall on the line between these end members, then the contaminant must be of a different source than the plotted end member used to construct the mixing curve. As the mixing curve shows, when only 1% of the mixture is composed of high concentrations of Sr (flowback) with relatively high $^{87}Sr/^{86}Sr$, the $^{87}Sr/^{86}Sr$ of the now contaminated sample (aquifer) shows a dramatic increase in its $^{87}Sr/^{86}Sr$. This method can then be used to potentially attribute or dismiss a claim that hydraulic fracturing activities lead to the contamination of an aquifer.

No clear distinction can be made between the two analyzed aquifers based on their $^{87}Sr/^{86}Sr$ ratios (Fig. 5-5). It is possible that making a determination on any potential trends of the $^{87}Sr/^{86}Sr$ values of the aquifers is hindered by the small number of analyzed samples. Interestingly, concentrations of Sr from the Trinity aquifer are slightly elevated over the Woodbine aquifer. Four of the five samples from both aquifers are elevated over historical well data (Table 2-1) which were collected before hydraulic fracturing began in the area, prior to 1999. The aquifer samples analyzed for this research came from the Hildenbrand et al. (2015) data set, collected between 2013-2014. Fontenot et al. (2013) postulated that while there was no direct evidence that wells were contaminated by fluids

from hydraulic fracturing activity, a measureable increase in Sr concentrations had occurred in wells that were in proximity to fracking activities. This could have been caused by ground perturbations caused by the drilling activities itself which may have liberated scaling into the groundwater that had built up within the wells ([After Groat and Grimshaw, 2012]; Fontenot et al., 2013). Hildenbrand et al. (2015) subsequently resampled wells in the same area (analyzed in this study) after hydraulic fracturing activity decreased and found that overall Sr concentrations within these wells had decreased concurrently with the reduction in hydraulic fracturing activity. Though Hildenbrand determined that Sr concentrations decreased relative to the Fontenot data set, Sr concentrations for still elevated over historical levels showing that residual effects from hydraulic fracturing are still evident in the aquifer samples.

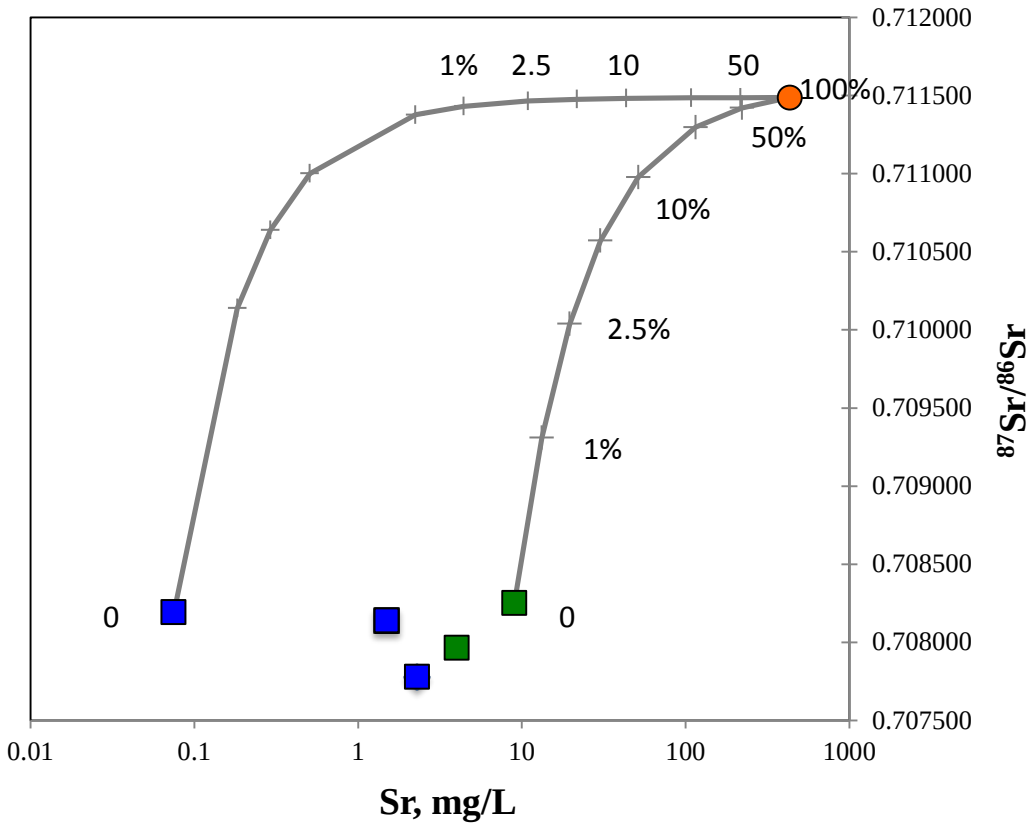

Figure 5-5 Mixing line between flowback and aquifer end members. The effect on the $^{87}Sr/^{86}Sr$ of an uncontaminated aquifer sample is displayed at varying concentrations of flowback where numbers along the curve represent the ratio of the flowback to aquifer components of the mixture. Blue squares are Woodbine Aquifer samples, green squares are Trinity Aquifer samples and the orange circle is flowback. Errors on the $^{87}Sr/^{86}Sr$ measurements are less then symbol size.

Chapter 6

Conclusions

$^{87}Sr/^{86}Sr$ can be a valuable measure to determine the provenance of dissolved solids. A flowback sample from hydraulic fracturing activities within the Barnett Shale and aquifer samples from private drinking wells in proximity to hydraulic fracturing activities were measured for elemental concentrations and their ratio of $^{87}Sr/^{86}Sr$. Powdered samples from the Barnett Shale were subjected to a sequential leaching procedure to determine the $^{87}Sr/^{86}Sr$ of different mineral phases and to see if the Sr radiogenic signature of the flowback sample could be reproduced from the leachates, in particular the H_2O leachate.

The major findings of the study include:

1. The sequential leachates of the Barnett Shale (H_2O, ammonium acetate, acetic acid, and hydrochloric acid) are composed of distinct mineral phases with geochemically and isotopically distinct values. Sodium (Na) was found primarily in the water soluble leach, potassium (K) and barium (Ba) was primarily within exchangeable cations, calcium (Ca) and strontium (Sr) were found in both exchangeable sites and carbonate, and magnesium (Mg) was found primarily in the carbonate and hydrochloric acid (HCl) soluble leaches. Excluding the ammonium acetate leach, a general trend among all core samples can be seen with decreasing $^{87}Sr/^{86}Sr$ from the H_2O to acetic acid leach, then increasing from the acetic acid leach to the HCl soluble fraction. A comparison of $^{87}Sr/^{86}Sr$ of the acetic acid leach to expected Mississippian marine

carbonates shows a significant difference. This is most likely attributed to diagenesis and the introduction of externally derived fluids with higher $^{87}Sr/^{86}Sr$ to the formation.

2. The original hypothesis of the study that the $^{87}Sr/^{86}Sr$ of the H_2O leachate would be most representative of the flowback sample was not proven. The study is hindered by a lack of sufficient samples and knowledge of the precise origin of the flowback sample, thus tying the flowback and core samples in time and space was not possible. This is critical since $^{87}Sr/^{86}Sr$ can vary widely by location within the same geologic formation. In order to have a complete analysis, a flowback sample should be acquired from a particular location within a formation and then compared to sequential leaches of a core sample from the formation at that same location (region and depth).

3. A mixing curve between two end-members with distinct isotopic compositions is a valuable tool to determine whether interaction has occurred between an "uncontaminated" (aquifer) and a contaminant, namely produced/flowback water (PFW). Mixing between a fluid containing high concentrations of Sr (contaminant) with a sample containing low concentrations of Sr (uncontaminated) will impart a measureable change on the $^{87}Sr/^{86}Sr$ of the now contaminated sample (assuming the fluids have differing $^{87}Sr/^{86}Sr$ values). This becomes evident when the mixture is composed of very small amounts (as low as 1%) of the contaminated sample. The results of this study show a mixing curve with the acquired aquifer samples containing relatively low concentrations of Sr and low $^{87}Sr/^{86}Sr$ values and a flowback sample containing relatively high concentrations of Sr and high $^{87}Sr/^{86}Sr$ values produces a line that can determine if the source of a contamination event originated from PFW or some other source.

It would be valuable to perform future work related to this study. Having the ability to acquire a flowback sample and core samples from the same well site could provide a more accurate assessment of the ability to simulate the interaction of fracturing

fluid with a formation. Additionally, the ability to collect flowback samples over a period of time after drilling commences would show the evolution of $^{87}Sr/^{86}Sr$ over time, thus giving a more accurate representation of the geochemical and $^{87}Sr/^{86}Sr$ values of the contaminating agent. The ability to collect aquifer samples from private wells in an area prior to commencement of hydraulic fracturing activities would give an accurate baseline to determine whether a contamination event has occurred.

Appendix A

Extraction Chromatography Procedure (modified from Scher et al., 2014)

Preparing Samples for Sr Spec Columns:

- Dry down (evaporate) ___ ml of sample water equivalent to 1 µg Sr in Teflon vials.
- Reconstitute dried sample in 100 µL 8M HNO3. Ultrasonic if needed to completely dissolve sample (~10 minutes).

Sr Spec Column Method:

1. Place columns in 8N HNO3 overnight. (cleaning the empty columns)

2. Clean the resin with 0.005 M HNO3 several times (3 times)

3. Fill columns with 0.125 mL Sr Spec resin in 0.005 M HNO3. (~200 mL)

4. Wash columns with 600 µL of 0.005 M HNO3.

5. Conditioning the columns: with 200 µL of 8 N HNO3.

6. Load the sample onto the column (100 uL of 8N HNO3).

7. Wash with 2 ml of 8M HNO3
   for calibration: collect each 100 µL aliquot

8. Elute Sr with 1 ml of 0.005 M HNO3 <**COLLECT**>
   for calibration: collect each 100 µL aliquot

Appendix B

Sequential Extraction Procedure (modified from Chapman, 2011):

CT = 50 mL centrifuge tube

1) Add crushed material to CT

Water soluble salts and sulfates

2) Add 30 mL ultrapure water to CT
3) Shake for 24 hours
4) Centrifuge briefly
5) Pour into syringe and filter leachant into 60 mL polypropylene bottles
6) Add 20 mL ultrapure water to CT
7) Centrifuge briefly
8) Pour into syringe and filter leachant into 60 mL polypropylene bottles
9) Two 3 mL aliquots are taken from 60 mL bottle for pH and anion analysis
10) Add 1 mL ultrapure nitric acid added to 60 mL bottle

Exchangeable cations - clays

11) 30 mL 1N ultrapure ammonium acetate buffered to pH 8 added to CT
12) Shake overnight
13) Centrifuge briefly
14) Pour into syringe and filter leachant into 60 mL polypropylene bottles
15) Repeat 11-14 adding 20 mL instead of 30 mL to CT
16) Dry down PMP beaker at 100°C

Carbonate Minerals

17) 30 mL 8% ultrapure acetic acid added to CT
18) Repeat 12-14 and 16

Other acid soluble phases

19) 30 mL 0.1N ultrapure hydrochloric acid added to CT
20) Repeat 12-14 and 16

Transfer all dried down salts using 2% ultrapure nitric acid into bottles

References

Abouelresh, M.O. and Slatt, R.M., 2012, Lithofacies and sequence stratigraphy of the Barnett Shale in east-central Fort Worth Basin, Texas: AAPG Bulletin, v. 96, n. 1, p.1-22.

Al Salem, O., 2014, The subsidence evolution of the Forth Worth Basin in north central Texas, USA [Ph.D. thesis]: Arlington, The University of Texas at Arlington, 47 p.

Alfredo, K., Adams, C., Eaton, A., Robertson, A.J., Stanford, B., 2014, The potential regulatory implications of strontium: American Water Works Association, 13 p.

"Barnett Shale Information." *Barnett Shale Information.* TXRRC, 1/18/2016. http://www.rrc.state.tx.us/oil-gas/major-oil-gas-formations/barnett-shale-information/. 3/15/2016.

“Barnett Shale rig counts.” Baker Hughes, 12/2015. http://phx.corporate-ir.net/phoenix.zhtml?c=79687&p=irol-reportsother. 1/24/2016.

Bataille, C.P. and Bowen, G.J., 2012, Mapping $^{87}Sr/^{86}Sr$ variations in bedrock and water for large scale provenance studies: Chemical Geology, (304-305), p. 39-52.

Brantley, S.L., Yoxtheimer, D., Arjmand, S., Grieve, P., Vidic, R., Llewellyn, G.T., Abad, J., Simon, C., 2014, Water resource impacts during unconventional shale gas development: The Pennsylvania experience: International Journal of Coal Geology, 126 (2014), p. 140-156.

Brantley, S., 2015, Drinking water while fracking: Now and in the future: Groundwater, v. 53(1), p. 21-23.

Capo, R., Stewart, B., Rowan, E., Kolesar Kohl, C., Wall, A., Chapman, E., Hammack, R., Schroeder, K., 2013, The strontium isotopic evolution of Marcellus Formation produced waters: International Journal of Coal Geology, 126 (2014), p. 57-63.

Celia, M.A., Bachu, S., Nordbotten, J.M., Kavetski, D., Gasda, D., 2005, Modeling critical leakage pathways in a risk assessment framework: Representation of abandoned wells: Fourth annual conference on carbon capture and sequestration, DOE/NETL, May 2-5.

Chaudhuri, S. and Ale, S., 2013, Characterization of groundwater resources in the Trinity and Woodbine aquifers in Texas: Science of the total environment, (452-453), p. 333-348.

Chapman, E., Capo, R., Stewart, B., Kirby, C., Hammack, R., Schroeder, K., Edenborn, H., 2012, Geochemical and strontium isotope characterization of produced waters from marcellus shale natural gas extraction: Environmental Science &Technology, 46, p. 3545-3553.

Chapman, E., 2011, Fossil fuel related water-rock interaction in the Appalachian Basin, Pennsylvania and New York: A geochemical and strontium isotope investigation [Ph.D. thesis]: Pittsburgh, University of Pittsburgh, 112 p.

Considine, T.J., Watson, R.W., Considine, N.B., Martin, J.P., 2013, Environmental regulation and compliance of Marcellus shale gas drilling: Environmental Geoscience, 20, p.1-16.

Crook, R., Kulakofsky, D., Griffith, J., 2003: Tailor lightweight slurry designs to well conditions and productions plans, World Oil (10) 224.

Darrah, T., Vengosh, A., Jackson, R., Warner, N., Poreda, R., 2014, Noble gases identify the mechanisms of fugitive gas contamination in drinking-water wells overlying the Marcellus and Barnett Shales: PNAS, v. 111(39), p. 14076-14081.

Davies, R.J., Almond, S., Ward, R.S., Jackson R.B., Adams, C., Worrall, F., Herringshaw, L.G., Gluyas, J.G., Whitehead, M., 2014, Oil and gas wells and their integrity: Implications for shale and unconventional resource exploitation: Marine and Petroleum Geology, 56. p. 239-254.

Dennie, D.P., 2010, An integrated paleomagnetic and diagenetic investigation of the Barnett Shale and underlying Ellenburger Group carbonates, Fort Worth Basin, Texas [Ph.D. thesis]: Norman, University of Oklahoma, 211 p.

Denison, R.E., Koepnick, R.B., Burke, W.H., Hetherington, E.A., 1998, 1994 Construction of the Cambrian and Ordovician seawater $^{87}Sr/^{86}Sr$ curve: Chemical Geology, v. 152 (3-4), p. 325-340.

Denison, R.E., Miller, N.R., Scott, R.W., Reaser, D.F., 2003, Strontium isotope stratigraphy of the Commanchean Series in north Texas and southern Oklahoma: GSA Bulletin, v. 115; no. 6, p. 669-682.

"Difference between flowback and produced water," Schramm, E., *What is flowback and how does it differ from produced water?*. Institute for Energy and Environmental Research of Northeastern Pennsylvania Clearinghouse website, http:energy.wilkes.edu/205.asp, Posted March 2011. Accessed April 2016.

Faure, G., Mensing, T., 2005, Isotopes: Principles and Applications: Hoboken, John Wiley & Sons Inc., 896 p.

Fontenot, B., Hunt, L., Hildenbrand, Z., Carlton Jr., D., Oka, H., Walton, J., Hopkins, D., Osorio, A., Bjorndal, B., Hu, Q., Schug, K., 2013, An evaluation of water quality in private drinking water wells near natural gas extraction sites in the Barnett Shale formation: Environmental Science & Technology, 47, p. 10032-10040.

Godderis, Y., and Francois, L.M., 1995, The Cenozoic evolution of the strontium and carbon cycles: relative importance of continental erosion and mantle exchanges: Chemical Geology, 126, p. 169-190.

Groat, C.G., and Grimshaw, T.W., 2012, Fact-based regulation for environmental protection in shale gas development: Energy Institute, The University of Texas at Austin, 414 p.

Harden, R.W., 2004, Northern Trinity/Woodbine aquifer groundwater availability model: Texas Water Development Board, 391 p.

Hildenbrand, L.H., Carlton, D.D., Fontenot, B., Meik, J.M., Walton, J., Taylor, J., Thacker, J., Korlie, S., Shelor, C.P., Henderson, D., Kadjo, A.F., Roelke, C., Hudak, P.F., Burton, T., Rifai, H.S., Schug, K.A., 2015, A comprehensive analysis of groundwater quality in the Barnett Shale region: Environmental Science & Technology, Vol. 49 Issue 13, p. 8254-8262.

Holland, J.M., 2011, An exploration of the ground water quality of the trinity aquifer using multivariate statistical techniques [M.S. thesis]: Denton, The University of North Texas, 87 p.

Kelley, V.A., Ewing, J., Jones, T.L., Young, S.C., Deeds, N., Hamlin, S., Scanlon, B., 2014, Updated groundwater availability model of the northern Trinity and Woodbine Aquifers: Intera, volume 1, 990 p.

Loucks, R.G. and Ruppel, S.C., 2007, Mississippian Barnett Shale: Lithofacies and depositional setting of a deep-water shale-gas succession in the Fort Worth Basin, Texas: AAPG Bulletin, v. 91, no. 4, p. 579-601

McArthur, J.M., 1994, Recent trends in strontium isotope stratigraphy: Terra Nova, 6, p. 331-358.

Nordstrom, P.L., 1982, Occurrence, availability, and chemical quality of groundwater in the Cretaceous aquifers of north-central Texas: Texas Water Development Board, report 269, 66 p.

Osborn, S. G., Vengosh, A., Warner, N.R., Jackson, R.B., 2011, Methane contamination of drinking water accompanying gas-well drilling and hydraulic fracturing: Proc. Nat. Acad. Sci., 108(20), p. 8172-8176.

Peckham, R.C., Souders, V.L., Dillard, J.W., Baker, B., 1963, Reconnaissance investigation of the ground-water resources of the Trinity River Basin, Texas: Texas Water Commission

Peterman, Z. E., Thamke, J., Futa, K., Preston, T., 2012, Strontium isotope systematic of mixing groundwater and oil field brine at Goose Lake in northeastern Montana, USA: Applied Geochemistry, 27, p. 2403-2408.

Pollastro, R.M. Jarvie, D.M., Hill, R.J. Adams, C.W., 2007, Geologic framework of the Mississippian Barnett Shale, Barnett-Paleozoic total petroleum system, Bend arch-Fort Worth Basin, Texas: AAPG Bulletin, v. 91 (4), p. 405-436

"Price of oil." Nasdaq stock exchange, 1/25/2016. http://www.nasdaq.com/markets/crude-oil.aspx?timeframe=10y. 1/25/16]

Rostron, B. and Arkadakskiy, S., 2014, Fingerprinting "stray" formation fluids associated with hydrocarbon exploration and production: Elements, 10, p. 285-290.

Scher, H.D., Griffith, E.M., Buckley Jr., W.P., 2014, Accuracy and precision of $^{88}Sr/^{86}Sr$ and $^{87}Sr/^{86}Sr$ measurements by MC-ICPMS compromised by high barium concentrations: Geochemistry, Geophysics, Geosystems, v. 15, issue 2, p. 499-508.

"Shapefile of DFW Aquifers." *GIS Data.* Texas Water Development Board, 12/2006. https://www.twdb.texas.gov/mapping/gisdata.asp. 7/23/2015.

"Shapefile of Barnett Shale." US Energy Information Administration. http://www.eia.gov/pub/oil_gas/natural_gas/analysis_publications/maps/maps.htm#geodata. 7/23/2015.

"Shapefile of Texas counties." *Texas Counties.* ArcGIS, 12/24/2012. https://www.arcgis.com/home/item.html?id=05c3a3ad11cb4043a08238b510e55c35. 7/23/2015.

Stewart, B.W., Chapman, E.C., Capo, R.C., Johnson, J.D., Graney, J.R., Kirby, C.S., Schroeder, K.T., 2015, Origin of brines, salts and carbonate from shales of the Marcellus Formation: Evidence from geochemical and Sr isotope study of sequentially extracted fluids: Applied Geochemistry, (60), p. 78-88.

Torbergsen, H.E., Haga, H.B., Sangesland, S., Aadnoy, B.S., Saeby, J., Johnsen, S., Rausand, M., Lundeteigen, M.A., 2012: An introduction to well integrity, NorskOlje& Gas. Available. http://www.norskoljeoggass.no/en/Publica/HSE-andoperations/ Introduction-to-well-integrity/.

"Trinity Aquifer." *Trinity Aquifer.* Texas Water Development Board. https://www.twdb.texas.gov/groundwater/aquifer/majors/trinity.asp. 3/15/2016.

Turner, G.L., 1957, Paleozoic stratigraphy of the Fort Worth Basin:, *in* Conselman, F.B., ed., Study of the Lower Pennsylvanian and Mississippian rocks of the northeast Llano Uplift, Abilene and Fort Worth Geological Societies Joint Field Trip Guidebook, p. 57-77.

"Unconventional/conventional wells." U.S. Energy Information Administration, 5/31/2011. http://www.eia.gov/oil_gas/rpd/shaleusa1_letter.pdf. 8/15/2015.

Vengosh, A., Warner, N., Jackson, R., Darrah, T., 2013, The effects of shale gas exploration and hydraulic fracturing on the quality of water resources in the United States: Procedia Earth and Planetary Science, 7, p. 863-866.

Vengosh, A., Jackson, R., Warner, N., Darrah, T., Kondash, A., 2014, A critical review of the risks to water resources from unconventional shale gas development and hydraulic fracturing in the United States: Environmental Science and Technology, 48(15), p. 8334-8348.

Vidic, R.D., Brantley, S.L., Vandenbossche, J.M., Yoxtheimer, D., Abad, J.D., 2013, Impact of shale gas development on regional water quality: Science, vol. 340, p. 826-835.

Warner, N., Darrah, T., Jackson, R., Millot, R., Kloppmann, W., Vengosh, A., 2014, New tracers identify hydraulic fracturing fluids and accidental releases from oil and gas operations: Environmental Science and Technology, 48, p. 12552-12560.

Widanagamage, I.H., Schauble, E.A., Scher, H.D., Griffith, E.M., 2014, Stable strontium isotope fractionation in synthetic barite: Geochimica et Cosmochimica Acta, (147), p. 58-75

Xu, Y., Yang, Q., Li, Q., Chen, B., 2006: The Oil Well Casing's Anticorrosion and Control Technology of Changqing Oil Field, SPE 104445.

Biographical Information

Richard Brian Goldberg was born August 28, 1971 in Silver Spring, Maryland. He grew up in Danbury, Connecticut where he graduated from Danbury High School in 1989. Richard attended Hofstra University in Hempstead, NY where he earned his Bachelor of Business Administration in Accounting. He worked for 14 years in accounting and the IT field before purchasing a Dalworth Clean franchise which he ran for six years. At the expiration of the franchise contract, he returned to school to pursue a Master of Science in Environmental and Earth Sciences (Geoscience Thesis Option) under the supervision of Dr. Elizabeth Griffith. He is scheduled to complete his Masters degree in May of 2016 and hopes to enter industry as a geoscientist.